A Comprehensive Survey of Data Augmentation in Visual Reinforcement Learning

Guozheng Ma[1], Zhen Wang[2], Zhecheng Yuan[3],
Xueqian Wang[3], Bo Yuan[4,✉], Dacheng Tao[1,✉]

[1]Nanyang Technological University, [2]The University of Sydney,
[3]Tsinghua University, [4]The University of Queensland

GUOZHENG001@e.ntu.edu.sg
boyuan@ieee.org   dacheng.tao@ntu.edu.sg

October 22, 2024

Abstract

Visual reinforcement learning (RL), which makes decisions directly from high-dimensional visual inputs, has demonstrated significant potential in various domains. However, deploying visual RL techniques in the real world remains challenging due to their low sample efficiency and large generalization gaps. To tackle these obstacles, data augmentation (DA) has become a widely used technique in visual RL for acquiring sample-efficient and generalizable policies by diversifying the training data. This survey aims to provide a timely and essential review of DA techniques in visual RL in recognition of the thriving development in this field. In particular, we propose a unified framework for analyzing visual RL and understanding the role of DA in it. We then present a principled taxonomy of the existing augmentation techniques used in visual RL and conduct an in-depth discussion on how to better leverage augmented data in different scenarios. Moreover, we report a systematic empirical evaluation of DA-based techniques in visual RL and conclude by highlighting the directions for future research. As the first comprehensive survey of DA in visual RL, this work is expected to offer valuable guidance to this emerging field. A well-classified paper list that will be continuously updated can be found at this ⍟ GitHub site.

✉: Corresponding authors.

Contents

1 Introduction

Reinforcement learning (RL) addresses sequential decision-making problems in which an agent seeks to discover the optimal policy via trial-and-error interactions with the environment [1–4]. Visual RL, a variant that learns directly from visual observations such as images, has gained widespread application across various domains due to its intuitive and cost-effective approach to environmental perception [5, 6]. This paradigm has been successfully employed in video games [7], autonomous driving [8], robot control [9], and other areas. However, learning directly from high-dimensional visual observations remains largely hindered by the challenges of low sample efficiency and large generalization gaps [10, 11, 6, 12–15].

To learn sample-efficient and generalizable visual RL agents, a considerable amount of effort has been devoted to developing diverse approaches, including (1) applying **explicit regularization** techniques such as entropy regularization [16, 17] to constrain the model's weights [18–20]; (2) performing joint learning with RL loss and **auxiliary tasks** to provide additional representation supervision [6, 21–34]; (3) building a **world model** of the RL environment that allows learning behaviors from imagined outcomes [35–37, 11]; and (4) **pretraining an encoder** that can project high-dimensional observations into compact state representation [38–47].

Although these approaches have achieved remarkable success, they remain challenged by limited interaction data and poor sample diversity [12–14]. To address these limitations by increasing the quantity and diversity of training data, data augmentation (DA) has garnered increasing attention from the visual RL community in recent years [13–15, 23, 48]. As a data-driven method, DA is orthogonal to the aforementioned approaches and can be combined with them to further enhance performance [23, 49]. For instance, DA plays a crucial role in contrastive-based auxiliary tasks, injecting prior knowledge of task invariance [26, 38, 50]. In addition, DA is essential for pre-training a cross-task representation [38, 39]. Furthermore, various DA techniques, such as random cropping, have been incorporated into almost all visual RL algorithms as a form of data preprocessing [37, 31, 5].
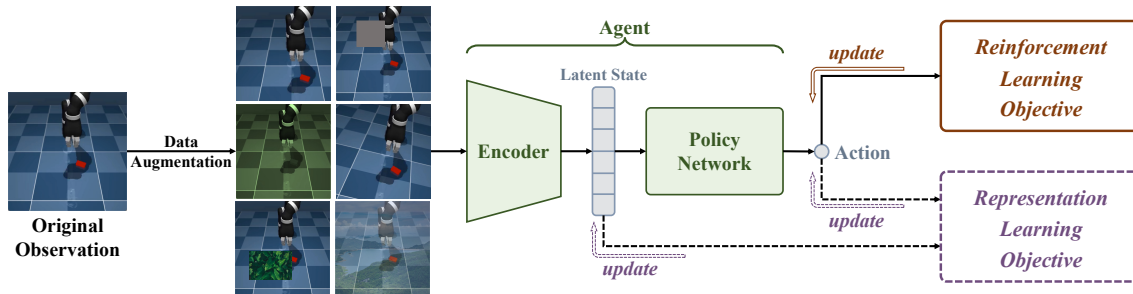
Figure 1: The generic workflow diagram for leveraging DA in visual RL.

In general, DA refers to strategies for generating synthetic training data from existing data without additional collection or interaction efforts [51, 52]. Figure 1 illustrates the generic workflow for leveraging DA in visual RL: diverse augmented data are generated by manipulating the original interaction data and then exploited to optimize the RL objective [12–14]. Moreover, DA can further enhance the representation learning in visual RL by incorporating auxiliary objectives [53, 54, 26, 23]. Despite the surge of related studies on leveraging DA in visual RL scenarios,

this fast-evolving and expanding field still lacks clarity and coherence. Therefore, this comprehensive survey aims to provide a bird's-eye view of DA-based methods in visual RL with the following main contributions:

1. Based on previous works [55, 56], we present High-Dimensional Contextual Markov Decision Process (HCMDP) as a general framework to formalize visual RL. This framework provides deep insights into the challenges of **low sample efficiency** and **large generalization gaps** in visual RL, which serve as the primary motivations for introducing DA.

2. We identify two key assumptions of DA with different motivations: the **optimality invariance** assumption for improving sample efficiency and the **prior-based diversity** assumption for narrowing the generalization gap.

3. We categorize related studies from two principled perspectives: **how to augment data** and **how to leverage augmented data** for improved clarity and coherence. This classification provides a structured framework for systematically reviewing existing work, offering a clear and logical organization of the field's current state.

4. We conduct **a unified empirical evaluation** of extensive DA-based methods on representative benchmarks to evaluate their sample efficiency and generalization abilities.

5. We present **an in-depth discussion** of the current landscape of DA in visual RL, forming the core of our survey. This section delves into the unique mechanisms of DA in this context, explores its significant challenges and opportunities, and provides crucial insights into both the present state and promising future directions of DA in visual RL.

Figure 2: The schematic structure of this survey.
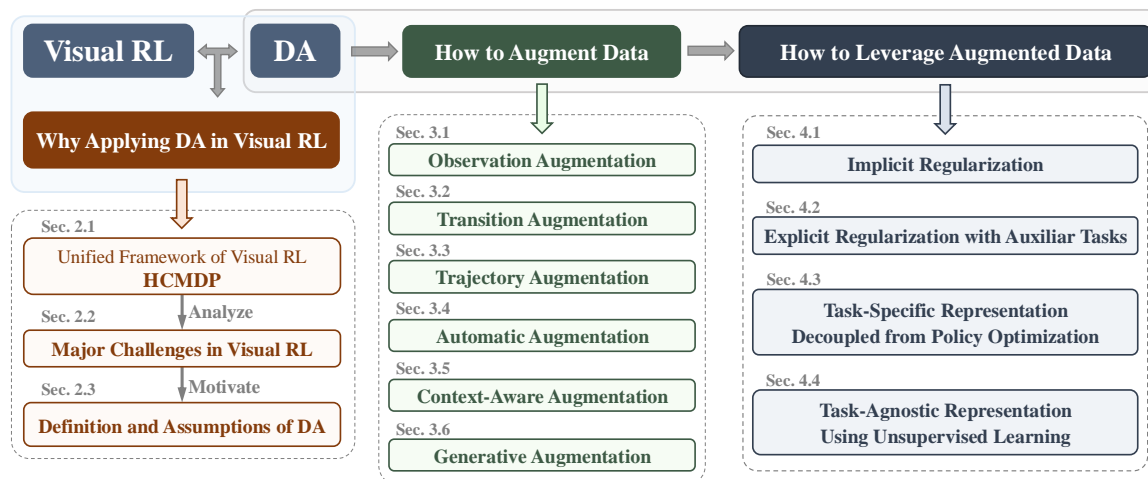
The body of this survey is organized as Figure 2. In Section 2, we propose a unified high-dimensional contextual Markov decision process (HCMDP) framework (Section 2.1) to formalize the visual RL scenario and highlight its major challenges (Section 2.2), as well as present the motivations and definitions of DA in visual RL (Section 2.3). We then conduct a systematic review

of the previous work from two perspectives: how to obtain and how to leverage augmented data in visual RL (Section 3 and Section 4). In Section 3, we categorize DA approaches in visual RL into *observation augmentation*, *transition augmentation*, and *trajectory augmentation*, based on the type of data each technique aims to modify. Moreover, we introduce three advanced extensions: *automatic augmentation*, *context-aware augmentation*, and *generative augmentation*. In Section 4, we present the different mechanisms used to leverage DA in visual RL, including implicit and explicit regularization, task-specific representation learning decoupled from policy optimization, and task-agnostic representation learning using unsupervised learning. To reveal the practical effect of DA, we introduce the typical benchmarks and summarize the empirical performance of recent DA-based methods in Section 5. In Section 6, we put forward a critical discussion concerning future research directions, including the opportunities, challenges, limitations, and underlying mechanisms of DA. Finally, this survey is concluded in Section 7 with a list of key insights.

Scope. Given the multitude of topics and research areas related to DA and visual RL, we constrain the scope of this survey in several ways to ensure its feasibility. • *Firstly*, this survey does not cover the related topic of domain randomization (DR) [57, 58], which aims to solve the sim-to-real problem in robot control by tuning the physical simulator's parameter distribution to align as closely as possible with reality [59–61]. In contrast, DA can only manipulate observations post-rendering, without access to the simulator's internal parameters, which affords it greater flexibility [55]. • *Secondly*, this survey focuses on scenarios that involve learning directly from visual inputs (visual RL) rather than handcrafted state inputs (state-based RL). Consequently, several works that introduce DA in state-based RL, will not be prominently featured in this survey [62, 63]. •*Thirdly*, while DA is a powerful tool, it is not the sole approach for improving sample efficiency and generalization in visual RL. To maintain coherence and focus, this survey does not provide detailed coverage of works that use DA as a foundational technique but whose primary research focus lies elsewhere[64, 65]. We strongly recommend readers interested in generalization issues in RL to refer to another comprehensive survey [55] that focuses on generalization in deep RL. •*Finally*, to ensure this survey aligns with the latest developments in AI field, we provide a detailed introduction to recent research on DA using advanced generative models in Section 3.6. Additionally, in Section 6.5, we critically examine the role and relevance of visual RL and DA in the context of the rapidly evolving landscape of foundation models.

2   Preliminaries

Visual RL addresses high-dimensional image observations instead of well-designed states and has encountered a series of new challenges [6, 13]. This section analyzes visual RL in depth and introduces the formalism of DA used for visual RL. In Section 2.1, we present a novel framework, HCMDP, to formalize the paradigm of visual RL. Based on this framework, we analyze the major challenges faced by visual RL in Section 2.2. Finally, Section 2.3 introduces the formalism of DA in visual RL, including its motivation, definition and two key assumptions.

2.1   High-Dimensional Contextual MDP (HCMDP)

The standard RL task is often defined as a **Markov Decision Process (MDP)** [2], which is specified by a tuple $\mathcal{M} = (\mathcal{S}, \mathcal{A}, r, \mathcal{P}, p, \gamma)$ where $\mathcal{S}$ is the state space; $\mathcal{A}$ is the action space; $r : \mathcal{S} \times \mathcal{A} \times \mathcal{S} \mapsto \mathbb{R}$ is the scalar reward function; $\mathcal{P}(s'|s,a)$ is the transition function; $p(\cdot)$ is the initial state distribution; and $\gamma \in (0,1]$ is the discount factor. The goal of RL is to learn an optimal policy $\pi^*(a \mid s)$ that maximizes the expected cumulative discounted return $\mathcal{R}(\pi, \mathcal{M})$, which is defined as:

$$\mathcal{R}(\pi, \mathcal{M}) = \mathbb{E}_{s_o \sim p(\cdot), a_t \sim \pi(\cdot|s_t), s_{t+1} \sim \mathcal{P}(\cdot|s_t, a_t)} \left[\sum_{t=0}^{\infty} \gamma^t r\left(s_t, a_t, s_{t+1}\right) \right] \tag{1}$$

Although the MDP is the standard paradigm of RL, it ignores a crucial factor of visual RL: agents only have direct access to high-dimensional observations instead of the actual state information. To properly formulate the visual RL scenarios, as shown in Figure 3, many variants of MDPs [66–69] have been introduced by using the high-dimensional observation space $\mathcal{O}$ to represent the image inputs. Depending on the specific assumptions, an emission function $\phi : \mathcal{S} \mapsto \mathcal{O}$ can be designed to simulate the mapping from the state space $\mathcal{S}$ to the observation space $\mathcal{O}$. For example, the (f, g)-scheme [56] constructs an emission function as the combination of generalizable and non-generalizable features while the contextual MDP (CMDP) [70, 69, 71, 55] introduces context c to distinguish contextual information from the underlying state information. However, these MDP variants mainly focus on how to explain the generalization effect in visual RL, and ignore the issue of constructing a compact representation from high-dimensional observations.

To better understand visual RL scenarios and provide a unified view of its specific challenges, we propose **High-Dimensional Contextual MDP (HCMDP)** as a general modeling framework of visual RL. Following the previous formalism [55, 56], the HCMDP $\mathcal{M}|_C$ can be defined as a family of environments:

$$\mathcal{M}|_C = \{\mathcal{M}|_c = (\mathcal{M}, \mathcal{O}_c, \phi_c) \mid c \sim p(c), c \in C\} \tag{2}$$

where $\mathcal{M} = (\mathcal{S}, \mathcal{A}, r, \mathcal{P}, p, \gamma)$ specifies the dynamics of the underlying system. With the fixed base MDP $\mathcal{M}$, the observation space $\mathcal{O}_c$ and emission function ϕ_c depend on the context c, which refers to the peripheral parameters that are not essential for agents to make decisions. $p(c)$ is the *context distribution*, and C represents the entire *context set*. For example, the colors and styles of backgrounds in robot scenarios are extraneous to control tasks, and are thus being referred to as task-irrelevant features.

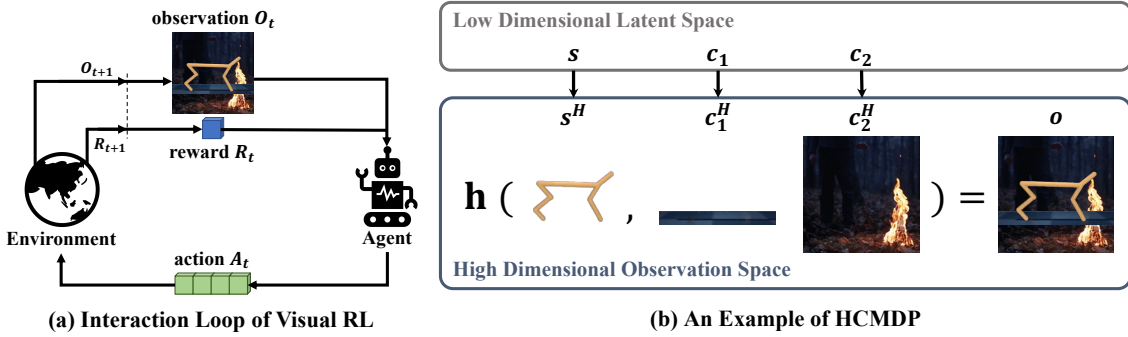**(a) Interaction Loop of Visual RL**   **(b) An Example of HCMDP**

Figure 3: The agent-environment interaction loop of visual RL and an example of HCMDP.

To be more specific, context c can be denoted as a set of parameters $\{c_1, c_2, \ldots, c_n\}$, where n is the number of task-irrelevant properties in this system. Each c_i corresponds to a task-irrelevant property, all of which are distributed over a fixed range: $\{c_1 \in C_1, c_2 \in C_2, \ldots, c_n \in C_n\}$. Consider an autonomous driving example such as CARLA [72]: an agent learns to control the car directly from pixels in changing environments. Therefore, the agent must distinguish between task-relevant and task-irrelevant components in the image observations. For instance, we can denote the style of the background buildings as c_1, the color of the driving car as c_2 and the number of people walking on the sides of the road as c_3.

The state s and context c constitute the complete information (parameters) used by the system to render the final observed images [56]. However, they both exist in the low-dimensional latent space, which cannot be directly observed. In fact, $\mathcal{O}$ is the only observable high-dimensional space where agents perceive task information. Following the assumptions [71, 56] that observations are high-dimensional projections of the state s and task-irrelevant contexts c, the emission function ϕ_c mapping from state $s \in \mathcal{S}$ to observation $o \in \mathcal{O}_c$ can be defined as:

$$o = \phi_c(s) := \mathbf{h}(s^H, c_1^H, c_2^H, \ldots, c_n^H) \tag{3}$$

where s^H is the high-dimensional representation mapped from the underlying state s, and each c_i^H is the high-dimensional representation uniquely determined by the latent context c_i. Similar to the formalism in [56], $\mathbf{h}$ is a "combination" function that combines the task-relevant state representation s^H and task-irrelevant context representations $(c_1^H, c_2^H, \ldots, c_n^H)$ to render the final observation. Based on the HCMDP framework, Figure 3 shows an illustration of a robot control environment from the DeepMind control suite [10]. In this scenario, contexts c_1 and c_2 separately denote the floor color and background style, respectively, which are both irrelevant to the control task. Correspondingly, c_1^H and c_2^H are the high-dimensional representations mapped from c_1 and c_2. The final observation o is the combination of the state representation s^H and the task-irrelevant representations c_1^H and c_2^H.

An HCMDP $\mathcal{M}|_C$ consists of a family of specific environments, where c follows the *context distribution* $p(c)$ over the entire *context set* C. In a given system, $\mathcal{M}$ and the rendering rules from s and c_i to the high-dimensional representations s^H and c_i^H are established. Hence, different combinations of the *context distribution* $p(c)$ and *context set* C produce different HCMDPs. For

any HCMDP $\mathcal{M}|_C$, the expected return of a policy is defined as:

$$\mathbf{R}(\pi, \mathcal{M}|_C) := \mathbb{E}_{c \sim p(c), c \in C}\left[\mathcal{R}\left(\pi, \mathcal{M}|_c\right)\right] \tag{4}$$

where $\mathcal{R}$ is the expected return of policy π in a specific MDP. In practice, we assume that the context distribution is uniform over the entire context set [55] so that different HCMDPs can be specified by their context sets $C = (C_1, C_2, \ldots, C_n)$. By choosing a training context set C_{train} and a test context set C_{test}, we can separately define the training context set HCMDP $\mathcal{M}|_{C_{\text{train}}}$ and the test context set HCMDP $\mathcal{M}|_{C_{\text{test}}}$. Agents are only allowed to be trained in $\mathcal{M}|_{C_{\text{train}}}$ and evaluated in the same HCMDP $\mathcal{M}|_{C_{\text{train}}}$ or HCMDP $\mathcal{M}|_{C_{\text{test}}}$, whose context exhibits a distribution shift from the training context set.

Remarks. The main difference between HCMDP and other MDP variants lies in the emission function $\phi : \mathcal{S} \mapsto \mathcal{O}$, as shown in Figure 4.

(a) HCMDP   (b) (f, g)-scheme   (c) Block MDP   (d) BC-MDP
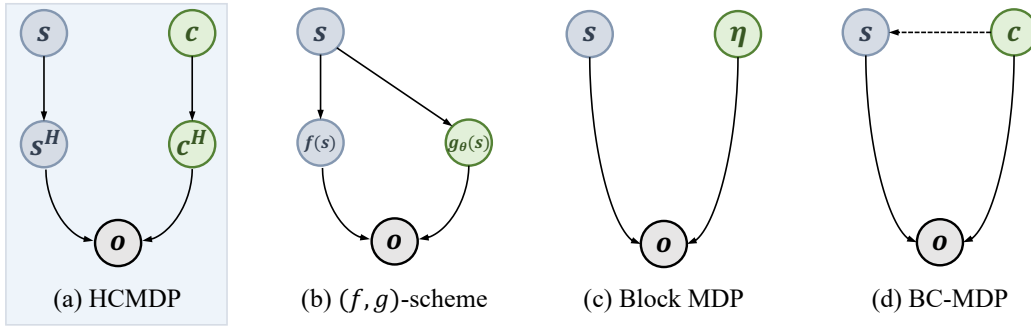
Figure 4: A graphical model of the emission function of a HCMDP (a) compared with three other representative MDP variants: (b) (f, g)-scheme [56], (c) Block MDP [73] and (d) BC-MDP [74].

First, the HCMDP highlights the high dimensionality of the observation space $\mathcal{O}$ by explicitly specifying the mapping between the latent variables s, c and their high-dimensional representations s^H, c^H. Second, it presents a unified perspective to understand the challenges of generalizing learned policy to unseen visual environments based on existing assumptions [56, 73, 74]. Specifically, the HCMDP assumes that the task-relevant features of state s and the task-irrelevant features of context c are combined in the final observation without further assumptions about their relationship. In the training process, agents tend to overfit the irrelevant context features and cannot effectively generate to unseen environments. As a general framework, the HCMDP can be transformed to other feasible MDP variants by making additional assumptions. For example, (f, g)-scheme [56] assumes that the unimportant features that do not contribute to extra generalizable information in observations are projected from the latent state with function $g_\theta(\cdot)$ dependent on the sampled parameter θ; Block MDP [73] assumes that the emission function is the concatenation of the noise and state variables as $s \oplus f(\eta)$, where η denotes spurious noise; and BC-MDP [74] assumes that the agent only has access to a partial state space $\mathcal{S}^c$, determined by the context c. By contrast, the HCMDP ignores the specific relationship between task-relevant and task-irrelevant features, focusing instead on the compound of these components.

Note that the HCMDP framework does not take into account the partially observable features of the underlying states in a partially observable MDP (POMDP) [75]. Following [2, 39, 13], we assume that the complete state information can be reasonably constructed by stacking three consecutive previous image observations into a trajectory snippet [14]. In summary, the motivation of HCMDP is to emphasize the fact that the underlying state s is projected to the high-dimensional observation space along with the task-irrelevant information of context c. With this unified framework, the unique challenges of visual RL scenarios compared with standard RL can be clearly analyzed.

2.2 Major Challenges in Visual RL

Despite the success of visual RL in complex control tasks with visual observations, sample efficiency and generalization remain two major challenges that may lead to ineffective agents [23, 15, 48, 76, 77]. In this subsection, we present the formal definitions of sample efficiency and the generalization gap based on the HCMDP framework and discuss their mechanisms.

2.2.1 Sample Efficiency

This term measures how well the interaction data are leveraged to train a model [78]. In practice, we consider an agent sample-efficient if it can achieve satisfactory performance within limited environment interactions [13, 23]. In other words, the goal of sample-efficient RL is to maximize the policy's expected return during the training of HCMDP $\mathcal{M}|_{C_{\text{train}}}$ based on as few interactions as possible. The expected return of policy π in $\mathcal{M}|_{C_{\text{train}}}$ can be defined as:

$$J(\pi) := \mathbf{R}(\pi, \mathcal{M}|_{C_{\text{train}}}) \tag{5}$$

Instead of making decisions based on predefined features, agents in visual RL need to learn an appropriate representation that maps a high-dimensional observation $\mathbf{h}(s^H, c^H)$ to the latent space $\mathbf{h}(s, c)$ to obtain decision-critical information [23, 13, 12]. Since standard RL algorithms already require large amounts of interaction data [17], learning directly from high-dimensional observations suffers from prohibitive sample complexity [6].

One solution to the sample inefficiency problem in visual RL is by training with auxiliary losses, such as pixel or latent reconstruction [6, 21], future prediction [22–25] and contrastive learning for instance discrimination [26–29] or temporal discrimination [79, 30–33]. Meanwhile, several model-based methods explicitly build a world model of the RL environment in pixel or latent spaces to conduct planning [35–37, 11]. Recently, pretrained encoders have demonstrated great potential in downstream tasks where the visual RL environment is explored in an unsupervised manner to obtain a task-agnostic pretrained encoder that can quickly adapt to diverse downstream tasks [38–41]. In addition, applying the pretrained encoders from other domains such as ImageNet [80] to visual RL also has shown its efficiency in downstream tasks [43–46]. The aforementioned methods have significantly improved the sample efficiency of visual RL, but the lack of training data remains a fundamental issue, which can be effectively solved by DA. Moreover, abundant auxiliary tasks and world models are designed and trained based on the augmented data [26, 23, 24, 11]. Hence, DA plays a vital role in improving the sample efficiency of visual RL algorithms.

2.2.2 Generalization

An agent's generalization ability can be measured by the generalization gap when transferred to unseen environments, which has been extensively investigated [56, 66, 81] and reviewed [55]. For an HCMDP with varying context sets C_{train} and C_{test}, the generalization gap of policy π can be defined as:

$$\text{GenGap}(\pi) := \mathbf{R}(\pi, \mathcal{M}|_{C_{\text{train}}}) - \mathbf{R}(\pi, \mathcal{M}|_{C_{\text{test}}}) \tag{6}$$

As mentioned in Section 2.1, the task-relevant information of state s is often conflated with the task-irrelevant information of context c, which may cause agents to overfit the task-irrelevant components [56]. How to train generalizable agents across different environments remains challenging in visual RL, and distinguishing between the task-relevant and task-irrelevant components of the observed images is essential for narrowing the generalization gap.

A naive approach to enhancing generalization is to apply regularization techniques originally developed for supervised learning [18, 19], including ℓ_2 regularization [82], entropy regularization [16, 17], dropout [20] and batch normalization [83]. However, these traditional regularization techniques show limited improvement in generalization and may even negatively impact sample efficiency [18, 13, 83]. As a result, recent studies focus on learning robust representations to improve the agent's generalization ability by introducing bisimulation metrics [84, 85], multiview information bottleneck (MIB) [29], pretrained image encoder [42] etc. From an orthogonal perspective, DA has been effective in enhancing generalization by generating diverse synthetic data [12, 13]. Moreover, DA can implicitly provide prior knowledge to the agent as a type of inductive bias or regularization [55, 86]. A detailed elaboration of the generalization issue in RL is provided in [55], which systematically reviews the related studies.

2.3 DA in Visual RL

As discussed in Section 2.2, the quantity and diversity of training data are crucial for achieving sample-efficient and generalizable visual RL algorithms. DA, as a data-driven approach, has demonstrated significant potential for visual RL in terms of both sample efficiency and generalization ability [12–15, 48, 87, 38, 54]. The advantages of DA for visual RL can be viewed from two aspects: (1) it can significantly expand the volume of the original interaction data, thus improving the sample efficiency [12]; (2) it introduces additional diversity into the original training data, making agents more robust to variations and enhancing their generalization capabilities [55, 15]. Furthermore, theoretical foundations have also been developed for DA, such as invariance learning [88, 89] and feature manipulation [90]. Hence, DA has been well recognized as a viable solution for the challenges in visual RL [91, 55, 15]. Following the conventions in [13–15], we define a general augmentation $\tau : \mathcal{O} \times \mathcal{V} \mapsto \mathcal{O}^{aug}$ as a mapping from the original observation space $\mathcal{O}$ to the augmented observation space $\mathcal{O}^{aug}$:

$$o^{aug} \triangleq \tau(o; \nu) \qquad \forall o \in \mathcal{O}, \nu \in \mathcal{V} \tag{7}$$

where $\nu \in \mathcal{V}$ is a set of random parameters and $\tau(\cdot)$ is the transformation function acting on the observation o. To gain an intuitive understanding of the effect of DA, we identify two assumptions of $\tau(\cdot)$ corresponding to the challenges that DA seeks to address: the assumption of **optimality invariance** for improving the sample efficiency and the assumption of **prior-based diversity** for narrowing the generalization gap.

2.3.1 Optimality Invariance

In supervised learning (SL), DA methods usually assume that the model's output is invariant after transformations; therefore, they can be directly applied to labeled samples to produce supplementary data [51, 92]. Considering the property of RL, DrQ [13] defines the *optimality invariance* assumption as adding a constraint to the transformation τ, which induces an equivalence relation between state s and its augmented counterpart s^{aug} constructed from observations o and o^{aug}, respectively [15]. Hence, an optimality-invariant state transformation $\tau : \mathcal{O} \times \mathcal{V} \mapsto \mathcal{O}$ can be defined as a mapping that preserves the Q-values [15], V-values and policy π [54] :

$$Q(o,a) = Q(\tau(o;\nu),a), V(o) = V(\tau(o;\nu)) \text{ and } \pi(o) = \pi(\tau(o;\nu)) \quad \forall o \in \mathcal{O}, a \in \mathcal{A}, \nu \in \mathcal{V} \quad (8)$$

where ν is the set of parameters of $\tau(\cdot)$, drawn from the set of all possible parameters $\mathcal{V}$. Note that optimality invariance relies on strict restrictions on $\tau(\cdot)$ and the size of $\mathcal{V}$ to ensure that the same s can be constructed from the original and augmented observations. In the HCMDP framework, optimality invariance means that augmentation transformations only change the selected contexts in the high-dimensional observation space while preserving the entire (conceptual) state information in the latent space.

For instance, random cropping [12, 13] satisfies the optimality invariance assumption in most robot control environments such as the DeepMind control suite [10]. In Figure 5, cropping generates augmented observations by randomly extracting central patches from the original image. Since the robot is centrally placed in the images, cropping only eliminates irrelevant information such as the background color while preserving the task-relevant information such as the robot's posture [71].
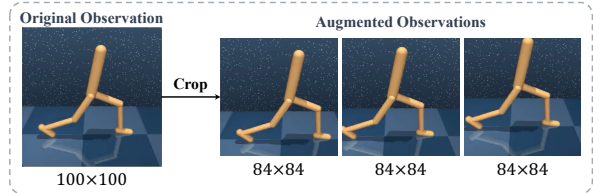
Figure 5: Optimality-Invariant augmentation.

With the optimality-invariant augmentation of the original observations, we can obtain sufficient training data based on limited interactions with the environment so that the sample efficiency can be significantly improved [13, 54]. However, due to the constraint of Eq. 8, optimality-invariant augmentations cannot provide sufficient diversity to enhance the agent's generalization ability [13, 15]. Consequently, it is necessary to break the limitation of optimality invariance to capture the variation between the training and test environments [15, 55].

2.3.2 Prior-Based Diversity

Based on the prior knowledge of the task-irrelevant contexts that vary between the training and test environments, targeted augmentations can be applied to effectively capture these variations [55]. Consequently, *prior-based diversity* can be introduced by modifying the corresponding features in the observed images. Note that DA can only manipulate the observed images and cannot directly change the distribution of the latent context. Figure 6 shows a typical scenario of DMControl-GB [53]. With the knowledge that the background color and style may vary when transferring the agent from training environments to test environments, we can purposefully employ augmentation techniques such as color jitter to diversify the color of the training observations [15]. By

developing an invariant policy or a latent representation from the prior-based strong augmentation (under the prior-based diversity assumption), the agents can successfully learn to identify these task-irrelevant features [55].
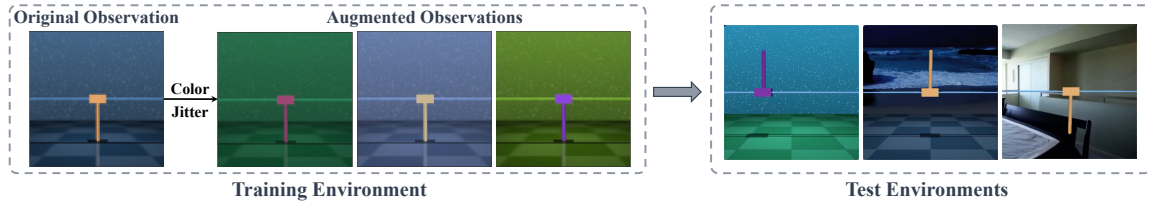
Figure 6: Examples of applying DA under the assumption of prior-based diversity.

Strong augmentation under the prior-based diversity assumption breaks the limitation of the optimality invariance assumption and therefore has tremendous potential for improving the agent's generalization ability. However, this approach inevitably increases the estimation variance of the Q-values and thus may harm the stability of the RL optimization process [15, 48].

3 How to Augment Data in Visual RL?

The aim of DA is to increase the amount and diversity of the original training data so that agents can learn more efficient and robust policies [15]. Thus, a primary focus of previous research was to design effective augmentation approaches [49, 24]. In this section, we introduce the mainstream augmentation techniques and discuss the pros and cons of these methods.
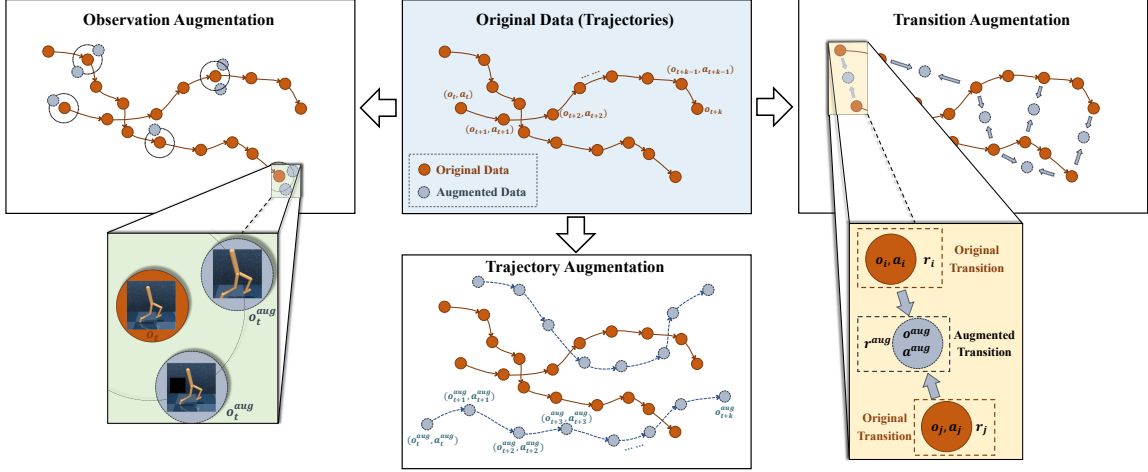
Figure 7: The comparison of different DA paradigms depending on the type of data augmented: **observation augmentation** only generates synthetic observations o_t^{aug}; **transition augmentation** augments observations together with supervision signals $(o_t^{aug}, a_t^{aug}, r_t^{aug})$; and **trajectory augmentation** generates virtual trajectories $(o_t^{aug}, a_t^{aug}, o_{t+1}^{aug}, a_{t+1}^{aug}, \ldots, o_{t+k}^{aug})$.

Based on the type of data being augmented, we categorize the DA approaches in visual RL into three main types, as illustrated in Figure 7 The first category, **observation augmentation**, involves transforming the given observations while keeping other transition factors (e.g., actions and rewards) unchanged, similar to label-preserving perturbations in SL. In Section 3.1, we detail various methods for employing DA on observations, which include not only diverse classical image manipulations directly applied to observation inputs but also several examples of DA in the feature space. The other two types, **transition augmentation** and **trajectory augmentation**, specifically take into account the unique properties of RL to broaden the scope of augmentation. In Section 3.2, we introduce transition augmentation, which enhances observations along with supervision signals, such as rewards. Finally, in Section 3.3, we explore trajectory augmentation, focusing on generating synthesized sequential trajectories.

In addition to summarizing techniques for augmenting different data types, this section will also introduce three advanced DA techniques that enhance the diversity of DA and improve its overall effectiveness. **Automatic augmentation** aims to automatically select the optimal DA type based on the specific task (Section 3.4), and **task-aware augmentation** (Section 3.5) focuses on providing data diversity while preserving critical information within the data. Furthermore, in light of recent advancements in generative AI, contemporary research has explored the use of technologies such as GANs and diffusion models for data generation; we will discuss this **generative augmentation** approach in Section 3.6.

3.1 Observation Augmentation

A typical observation augmentation approach is to apply the classical image manipulations to the observed images; most such manipulations were originally proposed for computer vision applications. Following the taxonomy of [51], we identify five categories of image manipulations: geometric transformations (Section 3.1.1), photometric transformations (Section 3.1.2), noise injections (Section 3.1.3), random erasing (Section 3.1.5) and image mixing (Section 3.1.4). Figure 8 shows a list of the visualized examples.
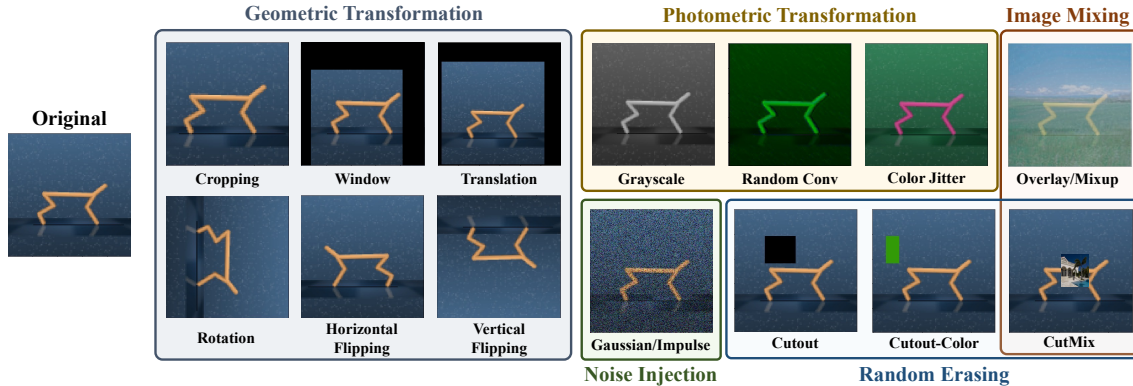
Figure 8: Visualized examples of observation augmentation via classical image manipulations.

3.1.1 Geometric Transformations

Geometric transformations are generally employed as optimality-invariant or label-preserving transformations [51] to overcome data shortages during the training process. **Random cropping** is an effective preprocessing technique for improving data efficiency; it works on image data with mixed width and height dimensions by locating a random central patch in each frame with a specific dimensionality [13, 14]. In many visual RL scenarios, such as robotic manipulation tasks, the vital regions are often positioned at the centers of the images, and cropping can remove irrelevant edge pixels to simplify the learning process [12]. Similar to cropping, the **window** transformation selects a random region and masks out the cropped part of the image, while **translation** renders the image with a larger frame and randomly moves the image within that frame.

Other forms of geometric transformation have also been introduced in visual RL scenarios. For example, **rotation** involves rotating an image right or left by r degrees, where r is randomly selected from a range [12]; **flipping** obtains additional data by flipping the observations horizontally or vertically. Although these techniques have been proven effective in computer vision tasks such as ImageNet [51], visual RL tasks are sensitive to angle information. In such a scenario, transformations such as rotation and flipping may produce erroneous results without properly adjusting the corresponding actions.

3.1.2 Photometric Transformations

In real-world applications, the colors of objects and backgrounds may vary due to conditions such as lighting and weather [93]. The intuition behind photometric transformations is to simulate

15

these color variations to prevent overfitting on the training data [94, 95]. Overfitting in visual RL is especially problematic due to the spurious correlations between task-irrelevant features and the agent's policy, which can severely damage its test performance [56]. Based on the prior knowledge concerning the variations between the training and test environments, photometric transformations aim to better generalize the agent's policy to unseen visual environments. For instance, **grayscale** simply converts images from RGB to grayscale [12], while **color jitter** varies the features of images that are commonly used in DA, including brightness, contrast, and saturation [96]. A common way to perform jitter in the color space is to convert images from RGB to HSV and add noise to the HSV channels [12]. Furthermore, **random convolution** has been introduced to mitigate visual bias that can negatively impact the performance of convolutional neural networks (CNNs) [97]. This technique augments image colors by passing the input observations through a randomly initialized single-layer convolutional network, which produces output layers of the same dimensions as the input.

3.1.3 Noise Injection

Adding noise to images can help CNNs learn robust features in computer vision tasks [98], and recent studies [15, 48] also attempted to exploit this mechanism in visual RL to obtain robust state representations. In practice, distortion can be introduced by adding **Gaussian** noise [12] or **impulse** (salt-and-pepper) noise [48].

3.1.4 Image Mixing

This type of methods is commonly used in computer vision tasks to improve a model's robustness and generalization ability [99]. Among the different versions of mixing, **Overlay/Mixup** [100] trains a neural network on the convex combinations of samples and their labels. In visual RL, there are two ways to leverage the Mixup mechanism. First, we can combine two observations and their supervision signals, which will be discussed in Section 3.2. Alternatively, we can mix RL observations and other images randomly sampled from another dataset while the supervision signals of the observations remain fixed. For example, SECANT [48] linearly blends an observation with a distracting image I as $f(o) = \alpha o + (1 - \alpha)I$, where I is randomly sampled from the COCO [101] image set.

3.1.5 Random Erasing

As an analog of the dropout regularization, erasing prevents the network from overfitting by working in the input data space instead of the network structure space [102]. **Cutout** [92] partially erases an image by randomly masking an $m \times n$ patch of the image. Furthermore, **Cutout-Color** masks the patch with a random color. As a combination of Cutout and Mixup, **CutMix** [103] replaces the removed region with a patch from another image and the supervision signals of the original observation are preserved (in visual RL scenarios) [48].

3.1.6 Feature Space Augmentation

Instead of applying DA in the input space, another effective approach to augment observations is to perform transformations in the feature space [104]. The feature space, also known as the latent

or embedding space, refers to an abstract domain that encodes meaningful internal representations from the original high-dimensional data.

The first approach to applying feature space augmentation typically involves autoencoders, which map input images to the latent feature space and then reconstruct the images based on the augmented features in that space. Common augmentations in the latent space include Gaussian noise addition and linear interpolation [105], which can generate more diverse datasets than traditional transformations in many supervised tasks [106, 107]. However, despite a few studies using autoencoders to design reconstruction-based auxiliary tasks to aid representation learning [6, 108], the use of autoencoders for generating high-quality augmented data has yet to be fully explored in visual RL scenarios.

Another approach is to extract representations from the lower layers of a CNN and directly augment the latent data without reconstructing the high-dimensional images [51]. For instance, MixStyle [109] adopts style mixing in the bottom layers to simulate various visual styles [110], and has demonstrated strong cross-domain generalization performance on benchmarks like Coin-Run [18]. More recently, CLOP [111] was introduced as an innovative augmentation technique that swaps pixel positions in the feature maps after the deepest convolutional layer while maintaining channel consistency. Experimental results show that CLOP significantly improves generalization performance without requiring additional representation learning tasks, due to the high-level abstract features contained in the deepest neural network layer.

3.2 Transition Augmentation

As shown in Figure 9, augmenting s_t with fixed supervision signals (e.g., the reward r_t and action a_t) can be regarded as a form of local perturbation of the corresponding transition, representing a key example of observation augmentation discussed in Section 3.1. To ensure the validity of the augmented transition $< s_t^{aug}, a_t, r_t, s_{t+1}^{aug} >$, the augmented observation s_t^{aug} must remain within a close range of the original observation s_t. Hence, local perturbation is inherently limited in terms of increasing data diversity, which is a common issue faced by all observation augmentations.
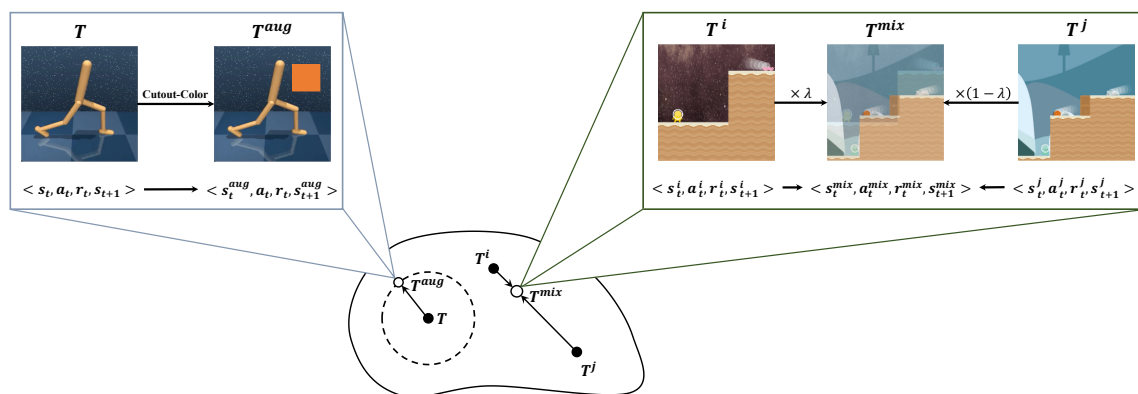

Figure 9: Comparison of observation augmentation and transition augmentation: observation augmentation via local perturbation (left, Cutout-Color [92]) and transition augmentation through joint interpolation of observations and supervision signals (right, MixReg [49]).

An intuitive solution is to apply interpolation across different data points instead of performing a local perturbation on each individual data point. Inspired by Mixup [100] and CutMix [103], MixReg [49] convexly combines two observations and their supervision signals to generate augmented data. For example, let y_i and y_j denote the signals for states s_i and s_j, respectively, which can be the reward or state values. After interpolating the observations by $\tilde{s} = \lambda s_i + (1 - \lambda)s_j$, MixReg introduces mixture regularization in a similar manner via $\tilde{y} = \lambda y_i + (1 - \lambda)y_j$, which helps learn more effective representations and smoother policies.

3.3   Trajectory Augmentation

Since observation or transition augmentation cannot directly enrich the trajectories encountered during training, to further improve the sample efficiency, PlayVirtual [24] augments the actions to generate synthesized trajectories under a self-supervised cycle consistency constraint.
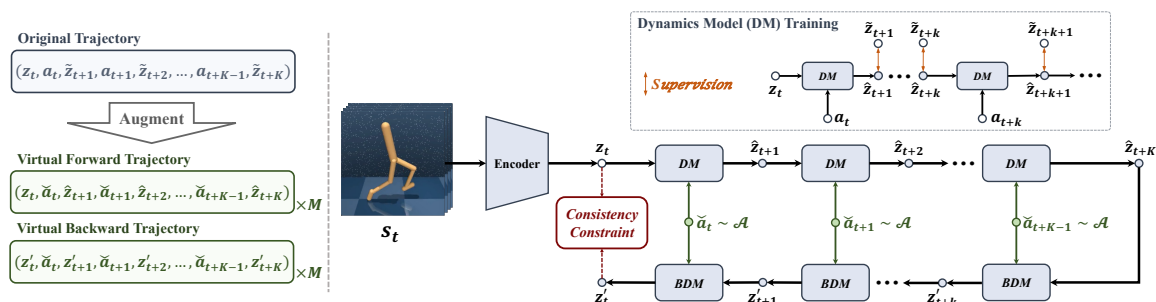
Figure 10: Data flow and architecture of PlayVirtual [24] as an example of trajectory augmentation.

In Figure 10, PlayVirtual operates entirely in the latent space after encoding the input observation s_t into a low-dimensional state representation z_t. Following the dynamics model (DM) in SPR [23], PlayVirtual introduces a backward dynamics model (BDM) to predict the backward transition dynamics $(z_{t+1}, a_t) \longrightarrow z_t$ to build a loop with the forward trajectory. During the training process, the DM is supervised by the original trajectory information, whereas the BDM is constrained by the cycle consistency between z_t and z'_t. Further discussion on how to train the dynamics models with the auxiliary loss will be provided in Section 4.2. After obtaining the effective DM and BDM, PlayVirtual can generate diverse synthesized trajectories by randomly sampling/augmenting M sets of actions in the action space $\mathcal{A}$ and then calculating the state information. Experimental studies confirmed that regularizing feature representation learning with cycle-consistent synthesized trajectories is the key to PlayVirtual's success.

3.4   Automatic Augmentation

Automatic augmentation is receiving increasing attention due to the demand for task-specific augmentations [112, 113, 96]. For example, although random cropping is one of the most effective augmentation techniques for improving sample efficiency on many benchmarks, such as DMControl-500k [12, 13] and Procgen [54], the induced generalization ability improvement heavily depends on the specific choice of augmentation strategy. In general, different tasks benefit from different augmentations, and selecting the most appropriate DA method often requires expert knowledge.

Consequently, it is crucial to develop methods that can automatically identify the most effective augmentation techniques. Research in visual RL remains in its early stages [54], and we highlight some promising approaches below.

Upper Confidence Bound (UCB): The task of selecting an appropriate augmentation from a given set can be formulated as a multi-armed bandit problem where the action space is the set of available transformations $F = \{f_1, f_2, \ldots, f_n\}$. The UCB [114] is a popular solution for the multi-armed bandit problem that considers both exploration and exploitation. Recently, UCB-DrAC [54] and UCB-RAD [115] were proposed to achieve automatic augmentation in visual RL. The experiment results suggest that UCB-based automatic augmentations can effectively improve the agent's generalization capabilities.

Meta Learning: Meta learning offers an alternative solution to automatic augmentation and can be implemented in two ways [54]: (1) training a meta learner, such as RL^2[116], to automatically select an augmentation type before each update in a DA-based algorithm; (2) meta-learning the weights of a CNN to perturb observed images, a technique similar to model-agnostic meta learning (MAML)[117, 118]. In practice, neither approach has yielded promising results, and designing expressive functions for automatic augmentation via meta learning remains a challenge.

3.5 Context-Aware Augmentation
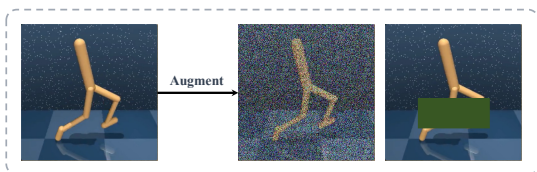
Figure 11: Context-agnostic DA may distort critical information in observations.

A notable limitation of existing DA techniques is their reliance on pixel-level image transformations that process each pixel without considering its contextual significance [87]. In the context of visual RL, however, pixels within an observation typically exhibit differential relevance to the decision-making process [119, 120]. As illustrated in Figure 11, context-agnostic augmentation techniques may inadvertently mask or alter critical regions in the original observation that are essential for decision making. This disregard for context elucidates why the straightforward application of prior-based strong augmentation, despite its potential to improve generalization, can significantly impair both sample efficiency and training stability in visual RL [15, 87]. This context-agnostic property explains why naively applying prior-based strong augmentation may severely damage both the sample efficiency and the training stability of visual RL, despite their potential to improve generalization [15, 87]. Consequently, incorporating context awareness into augmentation techniques is essential for enhancing the effectiveness of DA while minimizing its potential drawbacks. Currently, two viable approaches have been proposed to advance context-aware augmentation:

1. **Introducing human guidance.** Human-in-the-loop RL (HIRL) [121] is a general paradigm that leverages human guidance to assist the RL process. EXPAND [122] introduces a human saliency map to mark the importance levels of different regions, and it only perturbs the irrelevant regions. Saliency maps contain human domain knowledge, allowing context information to be embedded into the augmentation.

2. **Excavating task relevance.** In visual RL, the contextual information can be extracted from the task relevance of each pixel, making it possible to directly determine its task relevance to achieve context-aware augmentation. Task-aware Lipschitz DA (TLDA) [87] explicitly defines the task relevance by computing the Lipschitz constants produced when perturbing corresponding pixels. Regions with large Lipschitz constants are crucial for the current task decision, and these regions will subsequently be protected from augmentation.

Context-aware augmentation forms the foundation for semantic-level DA, which aims to apply targeted operations to different semantic contexts within observations [123, 87]. In Section 6.1, we will further discuss semantic-level DA as a challenging yet pivotal direction for future research.

3.6 Generative Augmentation

Despite the remarkable success of leveraging generative models for data augmentation in computer vision tasks [124–128], the application of VAEs or GANs to generate synthetic data for reinforcement learning has not only failed to achieve comparable performance but may even lead to detrimental effects [129, 130]. This limitation in visual RL remained unresolved until the recent emergence of diffusion models. A series of successful works leveraging diffusion models to generate high-quality synthetic data for visual RL have gradually emerged, marking a significant advancement in this field.

1. **Generative Augmentation for Observations.** ROSIE [131] and GenAug [132] leverage text-guided diffusion models to augment observations in robotic control tasks while preserving the corresponding actions, representing an advanced approach to observation augmentation using generative models. Trained on massive online datasets, the diffusion models employed for DA can zero-shot create realistic images of many different objects and scenes. This capability significantly expands the diversity of augmented observations beyond what is achievable with traditional DA transformations.

2. **Generative Augmentation for Transitions.** In contrast to approaches that solely generate observations, another line of research focuses on modeling the entire transition, simultaneously synthesizing novel action and corresponding reward labels. Within this paradigm, SynthER [133] directly trains diffusion models using either offline datasets or online replay buffers, subsequently generating samples for policy improvement. Advancing this concept further, MTDIFF [134] transcends the limitations of single-task scenarios by leveraging diffusion models to consolidate knowledge from multi-task datasets and augment data for novel tasks. The success of SynthER [133] and MTDIFF [134] demonstrates the significant potential of leveraging synthetic data to enhance visual RL performance.

Overall, recent studies and analyses indicate that data generated by diffusion models surpasses that of traditional DA methods in both diversity and accuracy [133]. This clearly demonstrates the capability of advanced generative models to produce novel, diverse, and dynamically accurate data. Such high-quality synthetic data can be effectively utilized by policies to enhance both the sample efficiency and generalization ability of visual RL algorithms. Furthermore, the text-controllable nature of current generative models enables them to serve as effective tools for semantically meaningful samples [132]. This capability holds promise for achieving genuine semantic-level manipulation of training data, presenting a crucial direction for future research.

3.7 Remarks

Data augmentation, as a data-centric approach, has demonstrated remarkable success in visual RL tasks, significantly enhancing both sample efficiency and generalization ability. This section provides a comprehensive review of various approaches addressing "How to augment data in visual RL". The key main takeaways can be summarized as follows:

1. In contrast to DA in supervised learning scenarios, visual RL tasks offer a wider varying range of manipulable data types [49, 24]. Among these, observation augmentation has gained the most widespread application due to its ease of implementation [14]. However, with the advancement of generative models, more complex yet diverse transition and trajectory augmentation techniques show potential for achieving novel breakthroughs.

2. To date, the most effective and widely adopted DA approaches for enhancing sample efficiency in visual RL are considered to be spatial perturbations and minor scaling of observations [135]. This finding notably diverges from conclusions in other domains, primarily due to the distinct underlying mechanisms through which DA significantly improves sample efficiency in visual RL [136]. We will discuss these mechanisms in depth in Section 6.3.

3. The robust generalization ability of visual RL agents during deployment largely depends on the diversity of training data. Consequently, both traditional strong augmentation techniques such as Color Jitter and advanced generative augmentation methods need to provide sufficient data richness to narrow the generalization gap [134]. In this context, ensuring training stability and maintaining the consistency of augmented data with environment dynamics become crucial considerations [87, 15].

4. The key to advancing DA in visual RL lies in automatically generating optimal and context-aware augmented data. Recent advancements in generative AI have opened up new possibilities for leveraging pre-trained generative models to produce novel data that is not only rich and diverse but also maintains the constraints of RL dynamics.

4 How to Leverage Augmented Data in Visual RL?

Next, we discuss how to exploit the augmented data in visual RL. To ease the discussion, we divide the application scenarios where DA plays a vital role into three cases.
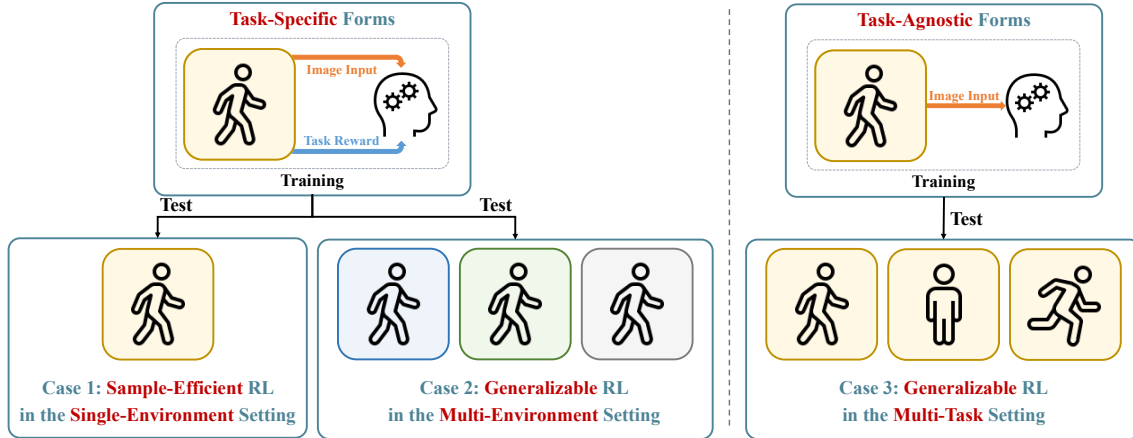
Figure 12: Three representative scenarios highlighting the critical role of DA. In the context of single-task environments, DA enhances sample efficiency during training and improves generalization ability during deployment. Furthermore, DA contributes to training task-agnostic representations, facilitating superior generalization and adaptation across multiple tasks.

Case 1 **Sample-efficient RL in the single-environment setting.** Agents are trained and evaluated within a fixed environment, commonly referred to as the single-environment setting [6]. The primary objective is to attain satisfactory performance with minimal interactions within the environment [13, 14, 135].

Case 2 **Generalizable RL in the multi-environment setting.** Agents are tested in unseen environments after interacting with the training environments [48]. Since RL agents tend to overfit the training environment [16], generalizing the learned policies to unseen environments remains challenging even when only visual appearances are altered [15, 137].

Case 3 **Generalizable RL in the multi-task setting.** Agents in the multi-task setting aim to adapt to different tasks. Traditional end-to-end RL algorithms heavily rely on task-specific rewards, making them unsuitable for other tasks [38]. Recent studies have attempted to address this limitation by pretraining cross-task representations in a task-agnostic manner, thereby enabling agents to swiftly adapt to multiple downstream tasks [138].

In Figure 12, RL agents are trained with task-specific rewards in Case 1 and Case 2, where DA is implemented as an implicit regularization penalty when enlarging the training set (Section 4.1). However, the effect of implicit regularization is limited [23], and many studies have attempted to design auxiliary losses to exploit the potential of DA (Section 4.2). Some studies have also aimed to decouple representation learning from policy optimization to attain more generalizable policies [48] (Section 4.3). Finally, the related works belonging to Case 3, referred to as task-agnostic representation approaches using unsupervised learning, are introduced in Section 4.4.

4.1 Implicit Policy Regularization

DNNs are capable of learning complex representational spaces, which is essential for tackling intricate learning tasks. However, the model capacity required to capture such high-dimensional representations makes these techniques difficult to optimize and prone to overfitting [139]. Moreover, the complexity of visual RL is further aggravated by the need to jointly learn representations and policies directly from high-dimensional observations based on sparse reward signals [6, 12]. As a result, it is difficult for agents to distinguish the task-relevant (reward-relevant) features from high-dimensional observations, and they may mistakenly correlate rewards with spurious features [56]. To solve these issues, researchers have conducted a series of studies to develop effective regularization techniques, which can prevent overfitting and improve generalization by incorporating the inductive biases of model parameters [139].

In RL, a myriad of techniques have been proposed as regularizers such as L^p-norm regularization [4], batch normalization [82], weight decay [18] and dropout [83]. Among them, L^p-norm regularization explicitly includes regularization terms as additional constraints, and is referred to as explicit regularization [56]. Conversely, weight decay and dropout aim to tune the optimization process without affecting the loss function, making them implicit regularization strategies [83]. Additionally, DA has been prevalent in the deep learning community as a data-driven technique [51, 86]. Furthermore, increasing efforts have been devoted to the theoretical underpinnings behind DA [140, 141, 90, 89, 142] to explain its regularization effects, including the derivation of an explicit regularizer to simulate the behaviors of DA [140].

The initial and naive practice of DA is to expand the training set with augmented (synthesized) samples [143]. This practice incorporates prior-based human knowledge into the data instead of designing explicit penalty terms or modifying the optimization procedure. Hence, it is often classified as a type of implicit regularization, formulated as the empirical risk minimization on augmented data (DA-ERM) [141] in SL tasks:

$$\widehat{h}^{da-erm} \triangleq \underset{h \in \mathcal{H}}{\arg\min} \sum_{i=1}^{N} l\left(h\left(\mathbf{x}_i\right), y_i\right) + \sum_{i=1}^{N} \sum_{j=1}^{\alpha} l\left(h\left(\mathbf{x}_{i,j}\right), y_i\right) \tag{9}$$

where $(\mathbf{x}i, y_i)$ represents the ith original training sample ($\mathbf{x}i \in \mathcal{X}$ denotes the input feature, and $y_i \in \mathcal{Y}$ is its corresponding label); $\mathbf{x}i, j$ signifies the jth augmented sample of $\mathbf{x}i$, which retains the corresponding label y_i; α indicates the number of augmentations; $l : \mathcal{Y} \times \mathcal{Y} \to \mathbb{R}$ is the loss function, and $h(\cdot)$ is the model to be optimized.

In the visual RL community, RAD [12] and DrQ [13] first leverage classical image transformation strategies such as cropping to augment the input observations via the implicit regularization paradigm. In the original paper, DrQ is proposed with two distinct ways to regularize the Q-function. On the one hand, it uses K augmented observations from the original s_i' to obtain the target values for each transition tuple (s_i, a_i, r_i, s_i'):

$$y_i = r_i + \gamma \frac{1}{K} \sum_{k=1}^{K} Q_\theta(f(s_i', \nu_{i,k}'), a_{i,k}'), a_{i,k}' \sim \pi(\cdot \mid f(s_i', \nu_{i,k}')) \tag{10}$$

where $f : \mathcal{S} \times \mathcal{T} \to \mathcal{S}$ is the augmentation function and ν is the parameter of $f(\cdot)$, which is randomly sampled from the set of all possible parameters $\mathcal{T}$. Alternatively, DrQ generates M

different augmentations of s_i to estimate the Q-function:

$$J_Q^{\mathrm{DrQ}}(\theta) = \frac{1}{NM} \sum_{i=1,m=1}^{N,M} ||Q_\theta(f(s_i, \nu_{i,m}), a_i) - y_i||_2^2 \tag{11}$$

In the above, DrQ leverages DA for improved estimation without adding any penalty terms, which is a type of data-driven implicit regularization. Since a sample can be defined as a tuple $(\mathbf{x}_i, y_i)$ in SL or a transition (s_i, a_i, r_i, s_i') in RL, the optimization objective of DrQ can be rewritten as:

$$J_Q^{\mathrm{DrQ}}(\theta) = \frac{1}{NMK} \sum_{i=1}^{N} \sum_{m=1}^{M} \sum_{k=1}^{K} l(f(s_i, \nu_{i,m}), a_i, r_i, f(s_i', \nu_{i,k}')) \tag{12}$$

where $l(s_i, a_i, r_i, s_i') = ||Q_\theta(s_i, a_i) - (r_i + \gamma Q_\theta(s_i', a_i'))||_2^2$ is the loss function, and $a_i' \sim \pi(\cdot \mid s_i')$. RAD [12] can be regarded as a specific form of DrQ with $K = 1$ and $M = 1$; it is a plug-and-play module that can be plugged into any RL method (on-policy methods such as PPO [3] and off-policy methods such as SAC [17]) without making any changes to the underlying algorithm. RAD has also highlighted the generalization benefits of DA on OpenAI Procgen [144].

Since RAD and DrQ directly optimize the RL objective on multiple augmented observation views without any auxiliary losses, they can be viewed as implicit approaches for ensuring consistency and invariance among the augmented views. Building on DrQ, DrQ-v2 [14] makes several algorithmic adjustments, such as switching the baseline from SAC to DDPG and employing a larger replay buffer, which has resulted in significantly improved sample efficiency. The success of DrQ-v2 demonstrates that when utilizing weak augmentation to achieve sample-efficient visual RL algorithms, the method of implicit regularization can effectively harness the benefits of DA.

(a) Q-Estimation Error (b) Action Distribution
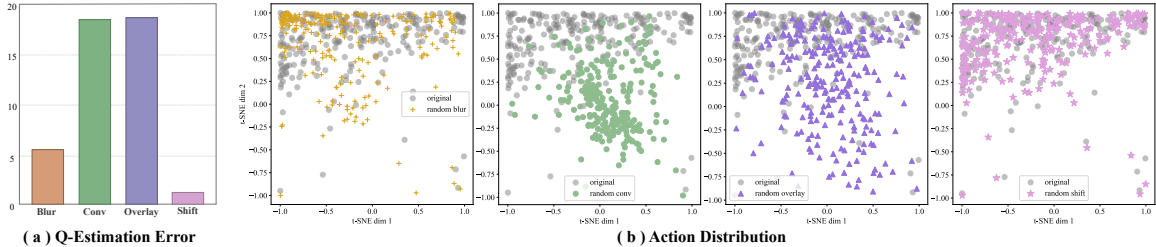
Figure 13: Q-**estimation errors and action distributions for augmented and original data.** (a) Mean absolute Q-estimation errors of the converged DrQ [13] agents for the same observations before and after augmentation (copied from [15]). (b) Action distributions between the augmented and original data. We use t-distributed stochastic neighbor embedding (t-SNE) to show the high-dimensional actions employed by the same converged DrQ agent.

However, later studies found that implicit regularization with cropping exhibits poor generalization performance in unseen environments [54, 15]. As discussed in Section 2.3, optimality-invariant transformations (represented by cropping) cannot provide sufficient visual diversity for reducing the generalization gap. Furthermore, although prior-based strong augmentations such as color jitter have the potential to improve generalization, they may induce large Q-estimation errors and action distribution shifts, as shown in Figure 13. Hence, implicit regularization approaches

with prior-based strong augmentations (e.g., random convolution and overlay) may make the RL optimization process fragile and unstable [15, 87]. This poses a *dilemma* in visual RL: diverse augmentation is necessary to improve an agent's generalization ability, but excessive data variations may damage the stability of RL [48].

SVEA [15] aims to enhance the stability of RL optimization with DA [13]. It consists of two main components. First, SVEA uses only original data copies to estimate Q-targets to avoid erroneous bootstrapping caused by DA, where $y_i = r_i + \gamma Q_\theta(s'_i, a'_i)$, $a'_i \sim \pi(\cdot \mid s'_i)$. Second, SVEA formulates a modified Q-objective to estimate the Q-value over both augmented and original copies of the observations, which can be expressed in a modified ERM form as follows:

$$
\begin{aligned}
J_Q^{\text{SVEA}}(\theta) &= \alpha \sum_{i=1}^{N} ||Q_\theta(s_i, a_i) - y_i||_2^2 + \beta \sum_{i=1}^{N} \sum_{m=1}^{M} ||Q_\theta(f(s_i, \nu_{i,m}), a_i) - y_i||_2^2 \\
&= \alpha \sum_{i=1}^{N} l(s_i, a_i, r_i, s'_i) + \beta \sum_{i=1}^{N} \sum_{m=1}^{M} l(f(s_i, \nu_{i,m}), a_i, r_i, s'_i)
\end{aligned}
\tag{13}
$$

For actor-critic algorithms, SVEA employs strong augmentation exclusively during critic updates, with no augmentation applied during actor updates. SVEA assumes that the encoder's output embedding can become fully invariant to input augmentations. Under this assumption, an actor trained solely on unaugmented observations can indirectly achieve robustness to augmented

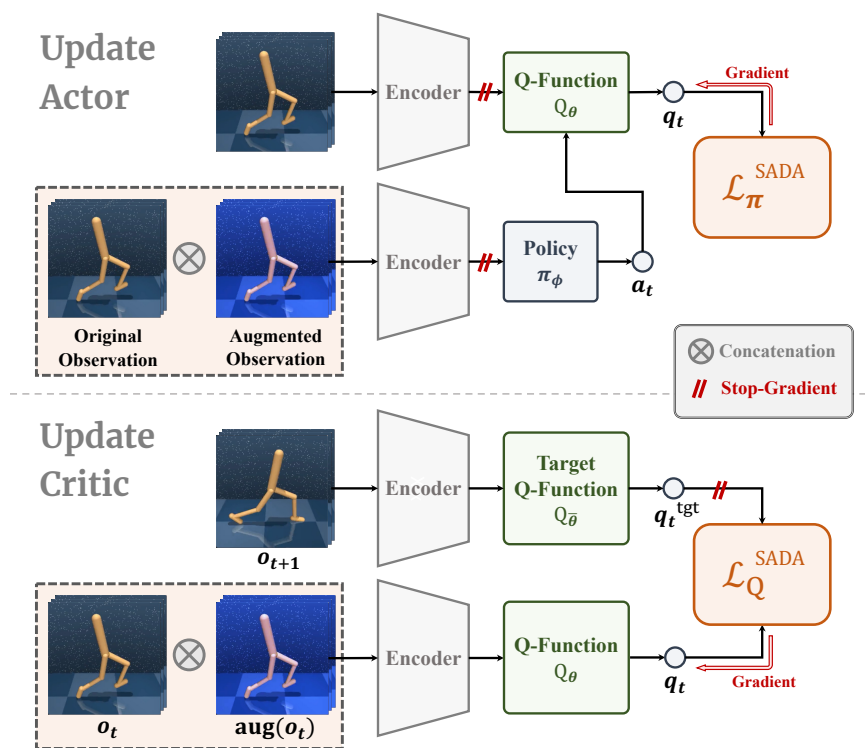Figure 14: The workflow of **S**tabilized **A**ctor-**C**ritic under **D**ata **A**ugmentation (SADA).

inputs via a shared actor-critic encoder. While this assumption holds for scenarios where the differences between test and training environments are limited to photometric changes, it fails when geometric augmentations are necessary for more complex generalization tasks.

To overcome this limitation, SADA [137] enhances the use of DA as implicit regularization to accommodate a broader range of augmentations. Instead of augmenting only the critic inputs, SADA carefully augments both actor and critic inputs to prevent training instabilities. As shown in the Figure 14, (1) during actor updates, only the policy input is augmented while the Q-function input remains unaugmented; (2) during critic updates, only the online Q-function input is augmented while the target Q-function input remains unaugmented; and (3) components are jointly optimized using both augmented and unaugmented data.

SVEA [15] and SADA [137] have significantly enhanced the generalization ability of visual RL algorithms. They achieve this by carefully designing pipelines that use strong augmentations without adding auxiliary losses or altering RL update mechanisms. This demonstrates the potential of implicit regularization to leverage DA for better generalization. However, it is crucial to meticulously design the use of strong augmentations to avoid training instabilities. In addition to carefully designing implicit regularization, other approaches have been explored to harness DA for improving both sample efficiency and generalization while avoiding adverse effects on training stability. These approaches include designing auxiliary tasks (Section 4.2) and decoupling representation learning from policy optimization (Section 4.3).

4.2 Explicit Policy Regularization with Auxiliary Tasks

Visual RL relies on the state representation, but it remains challenging to directly infer the ideal representation from high-dimensional observations [145]. A typical workflow involves designing auxiliary objectives to facilitate the representation learning process [146], or improve sample efficiency [26] or prevent observational overfitting [56]. In general, an auxiliary task can be considered an additional cost function that the RL agent predicts and observes from the environment in a self-supervised manner [147]. For example, the last layer of the network can be divided into multiple parts (heads), with each head dedicated to a specific task [34, 148]. These multiple heads then propagate errors back to the shared network layers, thereby forming the comprehensive representations required by all heads.

With the recent success in unsupervised learning, various auxiliary tasks have been designed to produce effective representations [147, 149]. Thus, it is natural to design additional losses to explicitly constrain an agent's policy and value functions, which we will discuss in Section 4.2.1. Moreover, we introduce contrastive learning as a lower bound of mutual information in Section 4.2.2 and future prediction objectives with a DM in Section 4.2.3.

4.2.1 DA Consistency

In contrast to simply inserting augmented data into the training dataset, DA consistency (DAC) [141] builds a regularization term to penalize the representation difference between the original sample $\phi_h\left(\mathbf{x}_i\right)$ and augmented sample $\phi_h\left(\mathbf{x}_{i,j}\right)$, under the assumption that similar samples should be

close in the representation space:

$$\underset{h \in \mathcal{H}}{\arg\min} \sum_{i=1}^{N} l\left(h\left(\mathbf{x}_i\right), y_i\right) + \lambda \underbrace{\sum_{i=1}^{N} \sum_{j=1}^{\alpha} \varrho\left(\phi_h\left(\mathbf{x}_i\right), \phi_h\left(\mathbf{x}_{i,j}\right)\right)}_{\text{DAC regularization}} \tag{14}$$

where ϕ_h refers to the features extracted from the high-dimensional data, which can be viewed as the output of any layer in the DNN, and ϱ is the metric function defined in the representation space, which can be the $\mathcal{L}_p$ norm or KL divergence. As an unsupervised representation module, DAC regularization can be employed as an auxiliary task in any SL or RL algorithms to enforce the model to produce similar predictions on the original and augmented samples. For example, SODA [53] calculates the consistency loss by minimizing the L^2 norm between the features of the augmented and original observations in the latent space; SIM [150] produces a cross-correlation matrix between two embedding vector sets of the original and augmented observations, and designs an invariance loss term to ensure the invariance of data.

For RL tasks, it is also desirable to train the network to output the same policies and values for both original and augmented observations [13]. For example, DrAC [54] employs two extra loss terms: G_π for regularizing the policy by the KL divergence measure and G_V for regularizing the value function using the mean-squared deviation:

$$G_\pi = KL\left[\pi_\theta(a \mid s) \mid \pi_\theta(a \mid f(s, \nu))\right], \qquad G_V = \left(V_\phi(s) - V_\phi(f(s, \nu))\right)^2 \tag{15}$$

The complete optimization objective of DrAC based on PPO is as follows:

$$J_{\text{DrAC}} = J_{\text{PPO}} - \alpha_r\left(G_\pi + G_V\right) \tag{16}$$

where α_r is the weight of the regularization term, and both G_π and G_V can be added to the objective of any actor-critic algorithm. By enforcing the DA consistency into the networks, specific transformations can be used to impose inductive biases relevant to the given task (e.g., invariance with respect to colors or translations) [54, 141].

Compared with implicit regularization techniques such as RAD and DrQ, DrAC employs two auxiliary consistency loss terms for explicitly regularizing the policy and the value function to ensure invariance. Instead of directly optimizing the RL objective on multiple augmented views of the observations, DAC regularization uses only the transformed observations $f(s, \nu)$ to compute the regularization losses G_π and G_V. Hence, DrAC can benefit from the regularizing effect of DA while mitigating the adverse effect on the RL objective [54].

4.2.2 Contrastive Learning

Another type of auxiliary task closely related to DA is contrastive learning. As **mutual information (MI)** is often hard to estimate, it is practical to maximize the lower bound of MI through approaches using, for example, InfoNCE loss [79]) to train robust feature extractors [151]. Recent studies [26, 38] have shown that contrastive learning can significantly improve the sample efficiency and generalization performance of visual RL [34]. Since contrastive learning only requires unlabeled data, it can not only be performed as auxiliary tasks together with RL objectives but also be leveraged to learn a task-agnostic representation, which we will discuss in Section 4.4.

27

In visual RL, there are two types of contrastive learning for improving agents' sample efficiency and generalization abilities [34]. The first class [26, 29, 28] focuses on **maximizing the MI between different augmented versions of the same observation** while minimizing the similarity between different observations. It tends to further exploit the regularization ability of DA at the MI level [34]. However, simply maximizing the lower bound of MI may retain the task-irrelevant information [152], which needs to be eliminated based on the information bottleneck principle. The second class [79, 38] aims to **maximize the predictive MI between consecutive states** by applying contrastive losses between an observation o_t and the near-future observations o_{t+k} over multiple time steps. This technique encourages the encoder to extract the temporal correlations of the latent dynamics from the observations [38], and DA can be applied as the prior-based data preprocessing.

Maximizing Multi-view MI: In self-supervised representation learning, feature extractors can be trained by maximizing the MI between different augmented views of the original data [151], and this approach has also been extended to the domain of visual RL [26, 27].
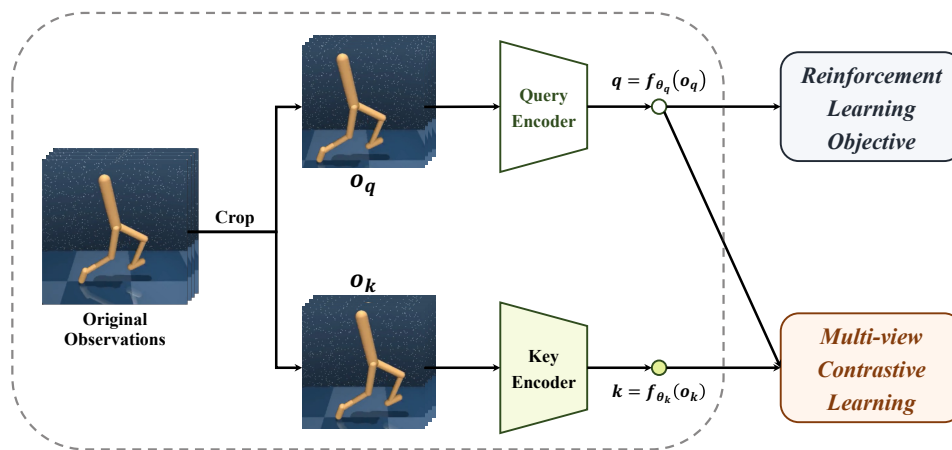
Figure 15: The workflow of **c**ontrastive **u**nsupervised **r**epresentations for **RL** (CURL).

CURL[26] is the first general framework for combining multi-view contrastive learning and DA in visual RL. It builds an auxiliary contrastive task to learn useful state representations by maximizing the MI between the different augmented views of the same observations to improve the transformation invariance of the learned embedding. In Figure 15, the contrastive representation is jointly trained with the RL objective, and the latent encoder receives gradients from both the contrastive learning objective and the RL objective.

A key component of contrastive learning is the selection of positive and negative samples relative to an anchor, and CURL uses instance discrimination rather than patch discrimination [26]. Specifically, the anchor and positive observations are two different augmentations of the same observation, while the negative samples come from other observations in the minibatch. The contrastive learning task in CURL aims to maximize the MI between the anchor and the positives while minimizing the MI between the anchor and the negatives.

Following the setting of momentum contrast (MoCo) [153], CURL applies DA twice to generate

queries and key observations, which are then encoded by the query encoder and key encoder, respectively. The query observations o_q are treated as the anchor, while the key observations o_k contain the positives and negatives. During the gradient update step, only the query encoder is updated, while the key encoder weights are set to the exponential moving average (EMA) of the query weights [153]. CURL employs the bilinear inner product $\text{sim}(q, k) = q^T W k$ to measure the agreement between query-key pairs, where W is a learned parameter matrix. Then, it uses the InfoNCE loss [79] to build an auxiliary loss function as follows:

$$\mathcal{L}_{\text{InfoNCE}} = \log \frac{\exp(q^T W k_+)}{\exp(q^T W k_+) + \sum_{i=0}^{K-1} \exp(q^T W k_i)} \tag{17}$$

where $\{k_0, k_0, \ldots, k_{K-1}\}$ are the keys of the dictionary and k_+ denotes a positive key. The InfoNCE loss can be interpreted as the log-loss of a K-way softmax classifier whose label is k_+ [151].

Many subsequently developed contrastive multi-view coding methods also employ the InfoNCE bound to maximize the MI between two embeddings that result from different augmentations. For example, DRIBO [29] aims to maximize the InfoNCE loss $\hat{I}_\psi(o_t^{(1)}, o_t^{(2)})$, where ψ represents the learnable parameters. Furthermore, ADAT [28] selects the positive observations with the same action type and the negatives with other actions so that more positives can be produced. CCLF [27] introduces a curiosity appraisal module to select the most informative augmented observations for enhancing the effect of multi-view contrastive learning.
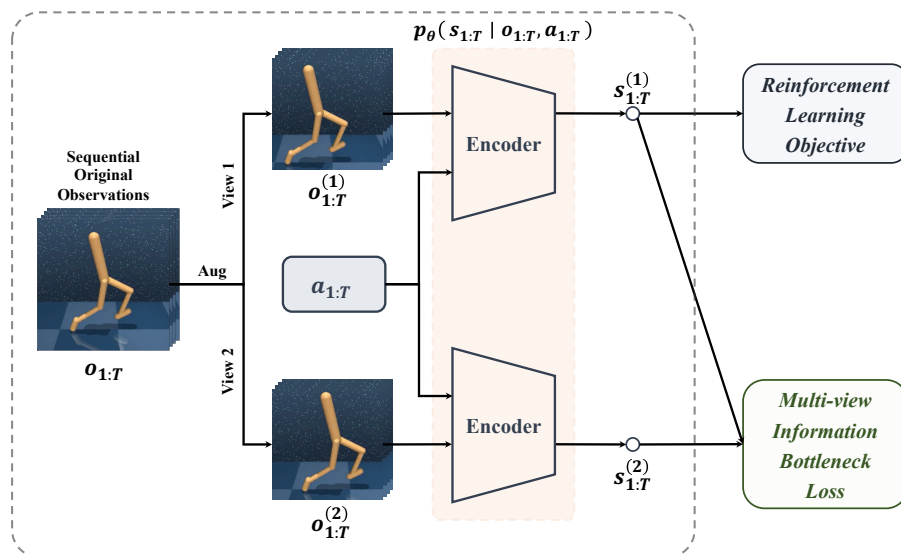
Figure 16: The workflow of **d**eep **R**L via multi-view **i**nfomration **bo**ttleneck (DRIBO).

Although maximizing the similarity between augmented versions of the same observation is valuable for state representation [26, 34], maximizing the lower-bound of MI may inevitably retain some task-irrelevant information, limiting the generalization abilities of agents. To tackle this issue, DRIBO [29] uses contrastive learning combined with a multi-view information bottleneck (MIB)-based auxiliary objective to learn representations that contain only task-relevant information that is predictive of the future while eliminating task-irrelevant information.

The assumption of DRIBO is that a desired representation for RL should facilitate the prediction of future states and discard excessive, task-irrelevant information from visual observations. In Figure 16, the augmented observations share the same task-relevant information, while any information not shared by them is regarded as being task-irrelevant [29]. In practice, the task-relevant MI can be maximized by InfoNCE, as in CURL. With the information bottleneck principle, DRIBO constructs a relaxed Lagrangian loss to obtain a sufficient representation with minimal task-irrelevant information, and the task-irrelevant minimization term is upper-bounded by:

$$\mathcal{L}_{\text{SKL}} = D_{\text{SKL}}(p_\theta(\boldsymbol{s}_t^{(1)} \mid \boldsymbol{o}_t^{(1)}, \boldsymbol{s}_{t-1}^{(1)}, \boldsymbol{a}_{t-1}) \,||\, p_\theta(\boldsymbol{s}_t^{(2)} \mid \boldsymbol{o}_t^{(2)}, \boldsymbol{s}_{t-1}^{(2)}, \boldsymbol{a}_{t-1})) \tag{18}$$

where D_{SKL} represents the symmetrized KL divergence based on the probability densities of $\boldsymbol{s}_t^{(1)}$ and $\boldsymbol{s}_t^{(2)}$ obtained using the encoder. Experiments have shown that DRIBO yields significantly improved generalization and robustness on the DeepMind control suite [10] and Procgen [144] benchmarks.

Maximizing Temporal Predictive MI: Another popular strategy for representation learning is to learn a compact predictive coding to predict future states or information, which can also be combined with DA. The first approach is to directly minimize the prediction error between the true future states and the predicted future states via a dynamic transition model, which will be discussed in Section 4.2.3. Another approach is to maximize the lower bound of the MI between the embeddings of consecutive time steps to induce predictive representations without relying on a generative model.

CPC [79] and ST-DIM [30] use temporal contrastive losses to maximize the MI between the previous state embedding and a future embedding several time steps later, but they both do not leverage DA to transform the observations. Recently, ATC [38], CCFDM [31] and CoDy [34] apply DA to regularize the observations obtained prior to encoding, imposing an inductive bias on information not relevant to the agent. For example, $\mathcal{L}_{\text{TMI}}$ in CoDy [34] aims to maximize the InfoNCE bound on the temporal MI between the embedding of the current state and action and the true embedding of the next state to increase the linearity of the latent dynamics. In practice, this approach first randomly draws a minibatch of transitions (s_t, a_t, s_{t+1}) from the replay buffer. Then, it obtains a minibatch of positive sample pairs (z_t^1, c_t, z_{t+1}) by feeding s_t, a_t and s_{t+1} into their corresponding encoders. For a given positive sample pair (z_t^1, c_t, z_{t+1}), it constructs negative samples by replacing z_{t+1} with all features z_{t+1}^* from other sample pairs $(z_t^{1*}, c_t^*, z_{t+1}^*)$ in the same minibatch. Furthermore, M-CURL [32] utilizes a bidirectional transformer to reconstruct the features of masked observations using information from surrounding observations. It then captures temporal dependencies by minimizing the contrastive loss between the reconstructed features and the original features.

4.2.3 Future Prediction with a DM

The motivation of future prediction tasks is to encourage state representations to be predictive of future states given the current state and future action sequence [34, 154, 155]. Instead of maximizing the MI between the current state and the future state using the InfoNCE loss [79, 30, 38], SPR [23] produces state representations by minimizing the prediction error between the **true future states** and the **predicted future states** using an explicit multi-step DM. As shown in Fig-

ure [17], this approach also incorporates DA into the future prediction task, which enforces consistency across different views of each observation.
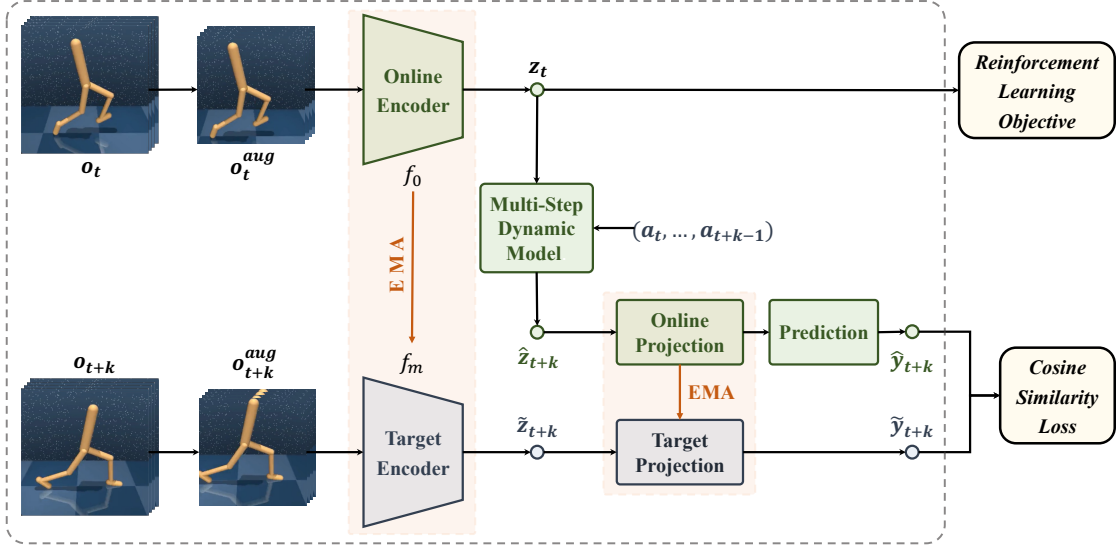

Figure 17: The workflow of **s**elf-**p**redictive **r**epresentations (SPR).

The DM $h(\cdot, \cdot)$ operates entirely in the latent space to predict the transition dynamics $(\mathbf{z}_t, a_t) \rightarrow \mathbf{z}_{t+1}$, where $\mathbf{z}_t = f(\mathbf{o}_t)$ is encoded by the feature encoder $f(\cdot)$ of the current input observation o_t. The prediction loss is computed by summing up the differences (errors) between the predicted representations $\hat{\mathbf{z}}_{t+1:t+K}$ and the observed representations $\tilde{\mathbf{z}}_{t+1:t+K}$:

$$\mathcal{L}_{\text{pred}} = \sum_{k=1}^{K} d\left(\hat{\mathbf{z}}_{t+k}, \tilde{\mathbf{z}}_{t+k}\right) = -\sum_{k=1}^{K} \left(\frac{\tilde{\mathbf{z}}_{t+k}}{\|\tilde{\mathbf{z}}_{t+k}\|_2}\right)^{\top} \left(\frac{\hat{\mathbf{z}}_{t+k}}{\|\hat{\mathbf{z}}_{t+k}\|_2}\right) \tag{19}$$

where the latent representation $\hat{\mathbf{z}}_{t+1:t+K}$ is computed *iteratively* as $\hat{\mathbf{z}}_{t+k+1} \triangleq h(\hat{\mathbf{z}}_{t+k}, a_{t+k})$, starting from $\hat{\mathbf{z}}_t \triangleq \mathbf{z}_t \triangleq f_o(o_t)$, and $\tilde{\mathbf{z}}_{t+k} \triangleq f_m(o_{t+k})$ is computed by the target encoder f_m, whose parameters are the EMAs of the parameters of the online encoder f_o. Combined with DA, SPR improves the agent's sample efficiency and results in superior performance with limited iterations on Atari Games and the DeepMind control suite [23].

PlayVirtual [24] is an extension of SPR that introduces cycle consistency to generate augmented virtual trajectories for achieving enhanced data efficiency. Following the DM in SPR [23], PlayVirtual [24] proposes a BDM for backward state prediction to build a cycle/loop with a forward trajectory. Given a DM $h(\cdot, \cdot)$, a BDM $b(\cdot, \cdot)$, the current state representation $\mathbf{z}_t$, and a sequence of actions $a_{t:t+K}$, a forward trajectory and the corresponding backward trajectory can be generated to form a synthesized trajectory:

$$\begin{aligned} &\textit{Forward}: \hat{\mathbf{z}}_t = \mathbf{z}_t, \hat{\mathbf{z}}_{t+k+1} = h\left(\hat{\mathbf{z}}_{t+k}, \mathbf{a}_{t+k}\right), \text{ for } k = 0, 1, \cdots, K-1 \\ &\textit{Backward}: \mathbf{z}'_{t+K} = \hat{\mathbf{z}}_{t+K}, \mathbf{z}'_{t+k} = b\left(\mathbf{z}'_{t+k+1}, \mathbf{a}_{t+k}\right), \text{ for } k = K-1, K-2, \cdots, 0 \end{aligned} \tag{20}$$

Since cycle consistency can be enforced by constraining the distance between the starting state $\mathbf{z}_t$ and the ending state $\mathbf{z}'_t$ in the loop, appropriate synthesized training trajectories can be obtained

by augmenting actions. In practice, the cycle consistency loss can be calculated by randomly sampling M sets of actions from the action space $\mathcal{A}$:

$$\mathcal{L}_{\mathrm{cyc}} = \frac{1}{M} \sum_{m=1}^{M} d_{\mathcal{M}} \left(\mathbf{z}'_t, \mathbf{z}_t \right) \tag{21}$$

where $d_{\mathcal{M}}$ is the distance metric over the latent space $\mathcal{M}$. The performance of PlayVirtual [24] can be explained from two aspects. First, the generated trajectories can help the agent "see" more flexible experiences. Second, enforcing the trajectory with the cycle consistency constraint can further regularize the feature representation learning process.

4.3 Task-Specific Representation Decoupled from Policy Optimization

Utilizing DA as an implicit [12, 13, 111] or explicit regularization approach with purposefully designed auxiliary tasks [26, 23, 34], the sample efficiency of visual RL has been significantly improved, resulting in performance comparable to state-based algorithms on several benchmarks [14]. However, training *generalizable RL agents* that are robust against irrelevant environmental variations remains a challenging task. Similar challenges in SL tasks, such as image classification, can be addressed by strong augmentations that heavily distort the input images, such as Mixup [100] and CutMix [103]. However, since the training process of RL is vulnerable to excessive data variations, a naive application of DA may severely damage the training stability [15, 48].

This poses a dilemma: aggressive augmentations are necessary for achieving good generalization in the visual domain [156], but injecting heavy DA into the optimization of an RL objective may cause deterioration in both the sample efficiency and the training stability [87]. Recent works [53, 48] argued that this is mainly due to the conflation of two objectives: policy optimization and representation learning. Hence, an intuitive idea is to decouple the training data flow by using nonaugmented or weakly augmented data for RL optimization while using strongly augmented data for representation learning. As shown in Figure 18, two strategies are available for achieving the decoupling goal: (1) dividing the training data into two streams to separately optimize $\mathcal{L}_{RL}$ and $\mathcal{L}_{SSL}$; and **iteratively** updating the model parameters by the two objectives [53]; (2) optimizing the RL objective $\mathcal{L}_{RL}$ first and then **sequentially** leveraging DA combined with SSL objective $\mathcal{L}_{SSL}$ for knowledge distillation [48].

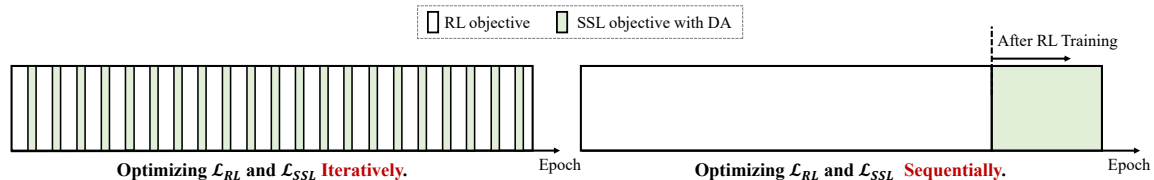Figure 18: Different strategies for decoupling policy optimization and representation learning.

Optimizing $\mathcal{L}_{RL}$ and $\mathcal{L}_{SSL}$ Iteratively: This strategy aims to divide the training data into two data streams and only uses the nonaugmented or weakly augmented data for the RL training process; it leverages strong augmentations under prior-based diversity assumptions to optimize

the self-supervised representation objective and enhance the generalization ability of the model. In practice, this technique can be performed by iteratively optimizing the RL objective $\mathcal{L}_{RL}$ and the self-supervised representation objective $\mathcal{L}_{SSL}$ in combination with DA to update the network parameters. For example, SODA [53] maximizes the MI between the latent representations of augmented and nonaugmented data as the auxiliary objective $\mathcal{L}_{\text{SODA}}$, and **continuously alternates** between optimizing $\mathcal{L}_{RL}$ with nonaugmented data and $\mathcal{L}_{\text{SODA}}$ with augmented data. While a policy is learned only from nonaugmented data, SODA still substantially benefits from DA through representation learning [53].

Optimizing $\mathcal{L}_{RL}$ and $\mathcal{L}_{SSL}$ Sequentially: This is a two-stage training strategy, which first trains a sample-efficient agent using weak augmentations, and then enhances the state representation by auxiliary self-supervised learning or imitation learning with strong augmentations. For example, SECANT [48] first trains a sample-efficient expert with random cropping (weak augmentation). In the second stage, a student network learns a generalizable policy by mimicking the behavior of the expert at every time step but with a crucial difference: the expert produces the ground-truth actions from unmodified observations, while the student learns to predict the same actions from heavily corrupted observations, as shown in Figure 19. The student optimizes the imitation objective by performing gradient descent on a supervised regression loss: $\mathcal{L}(o; \theta_s) = \|\pi_s(f(o)) - \pi_e(o)\|_F$, which has better training stability than the RL loss. Furthermore, conducting policy distillation through strong augmentations can greatly remedy overfitting so that robust representations can be acquired without sacrificing policy performance.
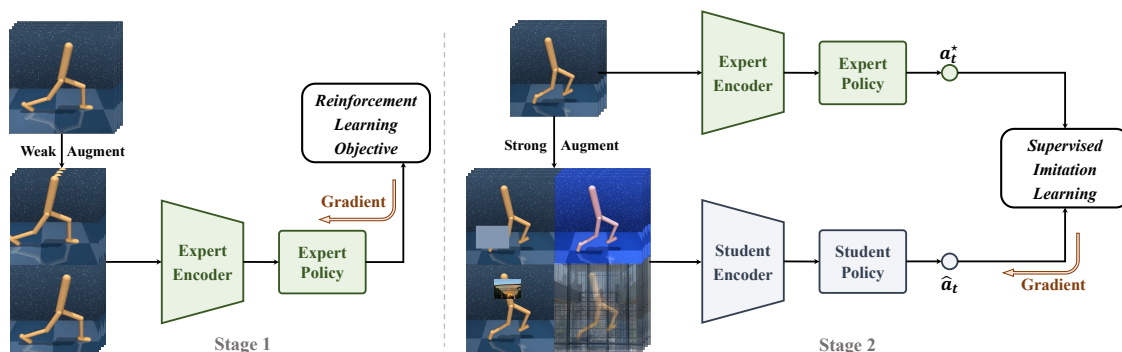
Figure 19: The workflow of **s**elf **e**xpert **c**loning for **a**daptation to **n**ovel **t**est-env (SECANT).

4.4 Task-Agnostic Representation Using Unsupervised Learning

Unsupervised/self-supervised pretraining, a framework that trains models without supervision, has achieved remarkable success in various domains [157–159] and can efficiently solve downstream tasks through fine-tuning. Similarly, it is also reasonable to learn an **unsupervised pretrained RL agent** that can quickly adapt to diverse test tasks in a zero-shot or few-shot manner [40, 43]. Furthermore, some recent studies [38] argued that the visual representations of standard end-to-end RL methods heavily rely on task-specific rewards, making them ineffective for other tasks. To overcome this limitation, the environment can be first explored in **a task-agnostic fashion to learn its visual representations** without any task-specific rewards, and

specific downstream tasks can subsequently be efficiently solved [38, 39]. Another key application of task-agnostic representation considers **multi-task settings** where, with the same or similar visual scenes, different downstream tasks are defined by corresponding reward functions. For instance, the *Walker* domain in the DeepMind control suite [10] consists of multiple tasks, including *standing*, *walking forward*, *flipping backward*, etc.

Two strategies are available for learning an encoder that maps a high-dimensional input to a compact representation in a task-agnostic fashion. The first approach is to design **unsupervised representation tasks**, as in Section 4.2. Second, we can **maximize the intrinsic rewards** to encourage meaningful behaviors in the absence of external rewards, which are derived from self-supervised forms such as the particle-based entropy and curiosity [160, 40, 39, 161, 162]. With the ability of DA to promote prior discrimination, many unsupervised pretraining studies combine DA with other auxiliary tasks to learn more meaningful representations. For example, ATC [38] applies random cropping combined with contrastive learning as the task-agnostic representation tasks, while APT [40] and SGI [162] leverage DA to design self-predictive tasks.

4.5 Remarks

As a data-centric method, DA is independent of specific RL baseline algorithms and can smoothly integrate with various techniques and training paradigms. When applied selectively to observations without altering other aspects of the algorithm, such as loss functions and training methodologies, DA acts as a form of implicit regularization. Conversely, incorporating auxiliary tasks to create a joint loss function while performing DA represents explicit regularization. In some auxiliary tasks, such as DA consistency regularization and multi-view contrastive learning, DA is an indispensable component. In other tasks, such as future prediction, DA serves as an enhancement. Furthermore, to mitigate training instability induced by strong augmentation, the decoupling of visual representation learning from policy optimization is receiving growing attention. This approach proves advantageous for both task-specific representations and general representations that are not tied to specific tasks.

The optimal approaches for maximizing the effectiveness of DA vary significantly across different scenarios. Based on recent studies, the most effective approaches to leveraging augmented data in the following three contexts are:

1. **Sample-efficient RL in the single-environment setting:** Weak augmentations, such as random shift, are considered the optimal type of DA for enhancing sample efficiency during training. The success of DrQ [13] and DrQ-v2 [14] demonstrates that using DA solely as an implicit regularization technique can significantly improve an agent's sample efficiency. Surprisingly, unlike in supervised learning, where DA typically provides incremental enhancements to training efficiency, DA can decisively influence the sample efficiency of visual RL algorithms [135]. Moreover, recent studies have demonstrated that DA alone can achieve more efficient performance compared to the meticulous design of self-supervised learning tasks [148] or the pre-training of representation encoders using additional data [163]. This unique phenomenon may be attributed to the different mechanisms through which DA facilitates sample-efficient visual RL, as opposed to traditional computer vision tasks. Further elaboration on this will be provided in Section 6.4.

2. **Generalizable RL in the multi-environment setting:** Strong augmentations based on priors, such as Color Jitter, are crucial for enhancing the generalization ability of visual RL. The key to leveraging strong augmentations lies in balancing their effectiveness while avoiding severe training instability. This trade-off will be discussed in detail in Section 6.2. Although SVEA [15] and SADA [137] have demonstrated that implicit regularization can handle strong augmentations through careful data flow design, employing specific representation tasks to utilize DA for generalization improvement is more conducive to maintaining training stability [23]. Additionally, decoupling representation learning from policy optimization has shown greater potential and should be considered the best practice for leveraging DA in this context [48, 53].

3. **Generalizable RL in the multi-task setting:** Combining DA with unsupervised learning is an effective strategy for training general visual representations, enabling agents to quickly adapt to multiple tasks. As the pre-training followed by fine-tuning paradigm gains popularity, there is growing interest in pre-training task-agnostic representations and subsequently developing efficient policies for specific tasks. Beyond training task-agnostic encoders from visual RL task observations using DA and unsupervised learning, leveraging diverse OOD vision data from other domains has shown greater potential for efficient adaptation to downstream tasks [43, 46, 45, 44, 164]. In Section 6.5, we will discuss the significance and necessity of DA in the context of pre-trained visual RL paradigms.

5 Experimental Evaluation

This section provides a systematic empirical evaluation of the methods in visual RL that leverage DA. First in Section 5.1, we introduce the commonly used benchmarks for evaluating the sample efficiency and generalization ability of agents. Then in Section 5.2 and Section 5.3, we present the experimental results of representative RL techniques using DA in comparison with those of other baselines to demonstrate the effectiveness of DA and identify the pros and cons of these methods.

5.1 Representative Benchmarks

5.1.1 Benchmarks for Sample Efficiency Evaluating in Visual RL

Atari Games [165]   This suite of games is widely used by both state-based and image-based discrete control algorithms for sample-constrained evaluations [2]. While RL algorithms can achieve superhuman performance on Atari games, they are still far less efficient than human learners, especially in image-based cases [26]. In the sample-efficient **Atari-100k** setting, only 100k interactions (400k frames with frame-skip=4) are available. The performance of an agent on a game is measured by its human-normalized score (HNS), defined as $\frac{S_A - S_R}{S_H - S_R}$ where S_A is the agent's score; S_R is the score of a random play; S_H is the expert human score.

DeepMind Control Suite [10]   This is a continuous control benchmark suite for evaluating visual RL algorithms. It presents a variety of challenging tasks, including bipedal balancing, locomotion, contact forces, and goal reaching, with both sparse and dense reward signals. Previous studies usually measured the data efficiency and performance of their algorithms on the DeepMind control suites with 100k (for measuring learning speed) and 500k (for measuring overall performance) environment steps, which are referred to as **DMControl-100k** and **DMControl-500k**, respectively. DeepMind control suite is also a proper testbed for multi-task settings, as different tasks often involve the same domain. For example, the walker domain contains running, walking, standing and many other tasks, allowing agents to transfer learned policies to other tasks with similar visual observations.

5.1.2 Benchmarks for Generalization Evaluating in Visual RL

Although Atari Games and the DeepMind control suite are suitable for benchmarking the sample efficiency of visual RL agents, they are not applicable for investigating the generalization abilities of these agents [12]. Generally, measuring the generalization ability of an agent requires variations between the training environment and the test environment, including state-space variations (the initial state distribution), dynamics variations (the transition function), visual variations (the observation function), and reward function variations [55]. In particular, DA-based techniques focus on zero-shot generalization to unseen environments with similar high-level goals and dynamics but different layouts and visual properties [15, 111, 166]. Figure 20 shows the representative benchmarks for evaluating the agent's generalization ability in visual RL.

OpenAI Procgen [144]   This is a suite of game-like environments where different levels feature varying visual attributes. Different combinations of the game levels can be used to separately
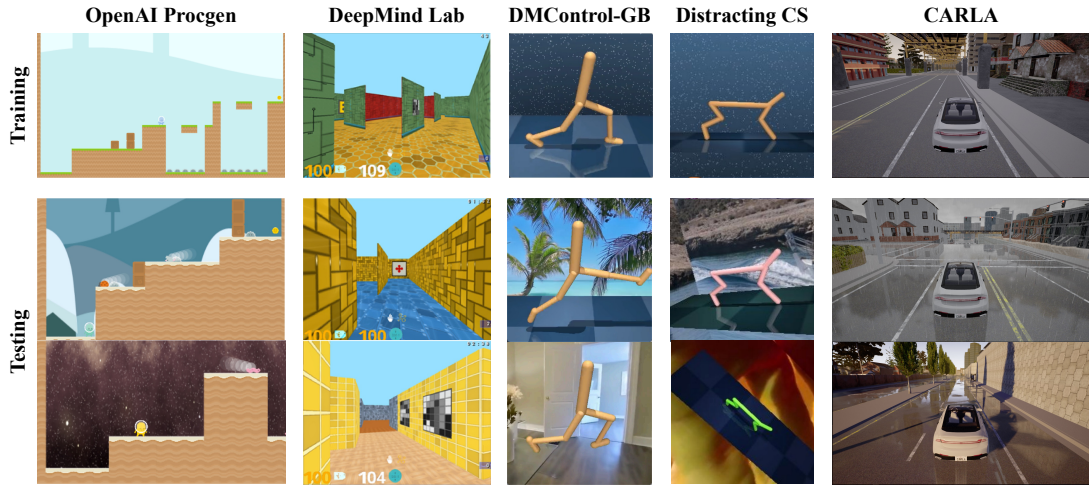
Figure 20: Typical benchmarks used to evaluate an agent's generalization ability in visual RL.

construct training and test environments. Agents are only allowed to be trained on limited levels and are evaluated on unseen levels with different backgrounds or layouts [49, 111].

DeepMind Lab [167]   This is a first-person 3D maze environment in which various objects are placed in the rooms. As a measure of their generalization ability, agents are trained to collect objects in a fixed map layout and tested in unseen environments that differ only in terms of their walls and floors (i.e., the variational contexts) [97].

DeepMind Control Suite Variants [168, 53, 55]   Since the original DeepMind control suite is not applicable for studying generalization, a number of variants have been proposed in recent years. Most of them, such as DMControl-GB [53], DMControl-Remastered [169] and Natural Environments [170], focus on visual generalization by changing the colors or styles of the background and floors. Furthermore, the Distracting Control Suite (DCS) [168] features a broader set of variations, including background style and camera pose variations.

CARLA [72]   This is a realistic driving simulator where the agent's goal is to drive as far as possible in 1000 time steps without colliding into 20 other moving vehicles or barriers [48]. Learning directly from the rich observations in this scenario is challenging since diverse types of task-irrelevant distractors (e.g., lighting conditions, shadows, realistic rain, clouds, etc.) are available around the agent, which increases the difficulty of extracting control-related features [171].

5.2   Sample Efficiency Evaluation

To measure the sample efficiency, we report the results on three common benchmarks: Atari-100k [165], DMControl-100k and DMControl-500k [10].

5.2.1 Atari-100k

In Table 1, the results of a random player (Random) and an expert human player (Human) are copied from [172] as baselines. Other scores are copied from their original papers [13, 27, 28, 32, 23, 24]. The results show that augmenting the observations as implicit regularization is effective, boosting the performance in terms of the median HNS from 5.8% (Efficient DQN) to 26.8% (DrQ). Moreover, appropriate auxiliary tasks such as contrastive learning [26, 32, 27, 28] and future prediction representation [23, 173, 24] can further yield improved sample efficiency. Among them, SPR [23] achieves the highest mean HNS value (70.4%) with its future prediction module, while PlayVirtual [24] achieves the highest median HNS value (47.2%) with the trajectory augmentation.

Table 1: **Evaluation of Sample Efficiency on Atari-100k.** We report the scores and the mean and median HNSs achieved by different methods on Atari-100k. The results are copied from the original works [13, 27, 28, 32, 23, 24].

Game	Human	Random	DQN [2]	CURL [26]	CCLF [27]	ADAT [28]	DrQ [13]	M-CURL [32]	SPR [23]	PlayVirtual [24]
Alien	7127.7	227.8	558.1	558.2	920.0	1029.7	771.2	**1151.6**	801.5	947.8
Amidar	1719.5	5.8	63.7	142.1	154.7	147.3	102.8	**182.2**	176.3	165.3
Assault	742.0	222.4	589.5	600.6	612.4	**749.4**	452.4	613.5	571.0	702.3
Asterix	8503.3	210.0	341.9	734.5	708.8	864	603.5	738.1	**977.8**	933.3
Bank Heist	753.1	14.2	74.0	131.6	36.0	164	168.9	220	**380.9**	245.9
Battle Zone	37187.5	2360.0	4760.8	14870.0	5775.0	21240	12954.0	**21600**	16651.0	13260.0
Boxing	12.1	0.1	−1.8	1.2	7.4	0.4	6.0	5.9	35.8	**38.3**
Breakout	30.5	1.7	7.3	4.9	2.7	4.5	16.1	5.7	17.1	**20.6**
Chopper Command	7387.8	811.0	624.4	1058.5	765.0	1106	780.3	**1138.9**	974.8	922.4
Crazy Climber	35829.4	10780.5	5430.6	12146.5	7845.0	21240	20516.5	20781.2	**42923.6**	23176.7
Demon Attack	1971.0	152.1	403.5	817.6	**1360.9**	851.9	1113.4	864.4	545.2	1131.7
Freeway	29.6	0.0	3.7	26.7	22.6	**29.7**	9.8	28.9	24.4	16.1
Frostbite	4334.7	65.2	202.9	1181.3	1401.0	1943.2	331.1	**2342.2**	1821.5	1984.7
Gopher	2412.5	257.6	320.8	669.3	**814.7**	601.2	636.3	453.8	715.2	684.3
Hero	30826.4	1027.0	2200.1	6279.3	6944.5	7259.2	3736.3	7360.6	7019.2	**8597.5**
Jamesbond	302.8	29.0	133.2	471.0	308.8	**635.7**	236.0	436.2	365.4	394.7
Kangaroo	3035.0	52.0	448.6	872.5	650.0	956.9	940.6	1691.4	**3276.4**	2384.7
Krull	2665.5	1598.0	2999.0	**4229.6**	3975.0	3502.9	4018.1	3240.9	3688.9	3880.7
Kung Fu Master	22736.3	258.5	2020.9	14307.8	12605.0	**19146**	9111.0	17645.6	13192.7	14259.0
Ms Pacman	6951.6	307.3	872.0	1465.5	1397.5	1075	960.5	**1758.9**	1313.2	1335.4
Pong	14.6	−20.7	−19.4	−16.5	−17.3	−15.1	−8.5	−8.9	−5.9	**−3.0**
Private Eye	69571.3	24.9	351.3	218.4	100.0	**388**	−13.6	321.6	124.0	93.9
Qbert	13455.0	163.9	627.5	1042.4	953.8	1578	854.4	1785	669.1	**3620.1**
Road Runner	7845.0	11.5	1491.9	5661.0	11730.0	12508	8895.1	12320	**14220.5**	13534.0
Seaquest	42054.7	68.4	240.1	384.5	550.5	251.6	301.2	481.1	**583.1**	527.7
Up N Down	11693.2	533.4	2901.7	2955.2	3376.3	3597.8	3180.8	4399.5	**28138.5**	10225.2
Mean HNS (%)	100	0	13.7	38.1	38.2	47.2	35.7	46.6	**70.4**	63.7
Median HNS (%)	100	0	5.8	17.5	18.1	20.6	26.8	34.0	41.5	**47.2**
# Superhuman	N/A	0	1	2	3	6	2	3	**7**	4
# SOTA	N/A	0	0	1	2	5	0	6	**7**	5

5.2.2 DMControl-100k and DMControl-500k

Compared with Atari games, the tasks in the DeepMind control suite [10] are more complex and challenging. We first report the performance of the underlying SAC algorithm [17] based on state and image inputs, referred to as Pixel SAC and State SAC in Table 2 (copied from [26]), respectively, followed by the results of SAC-AE [6]. Since State SAC operates on low-dimensional state-based features instead of pixels, it approximates the upper bounds of sample efficiency in these environments for image-based agents. Similar to the case of Atari-100k, DrQ [13] achieves significant improvements over the underlying SAC algorithm [17], which is unable to complete these tasks. Combining auxiliary tasks with DA provides improved performance and potential for training sample-efficient agents. For example, based on SPR [23], recent studies have achieved superior performance by introducing cycle consistency constraints for more diverse trajectories (PlayVirtual [24]) or curiosity modules for better exploration (CCFDM [31]).

Table 2: **Evaluation of Sample Efficiency on the DeepMind Control Suite.** The reported scores (means and standard deviations) are achieved by different methods on DMControl-100k and DMControl-500k. The results are copied from their original works with 10 random seeds [6, 26, 13, 23, 24, 27, 31, 34].

DMControl 100k	Pixel SAC	SAC-AE [6]	CURL [26]	DrQ [13]	SPR [23]	CCLF [27]	CoDy [34]	MLR [21]	CCFDM [31]	PlayVirtual [24]	State SAC
Finger,	179	747	767	901	868	**944**	887	907	880	915	811
Spin	±166	±130	±56	±104	±143	±42	±39	±58	±142	±49	±46
Cartpole,	419	276	582	759	799	799	784	806	785	**816**	835
Swingup	±40	±38	±146	±92	±42	±61	±18	±48	±87	±36	±22
Reacher,	145	225	538	601	638	738	624	**866**	811	785	746
Easy	±30	±164	±233	±213	±269	±99	±42	±103	±220	±142	±25
Cheetah,	197	252	299	344	467	317	323	**482**	274	474	616
Run	±15	±173	±48	±67	±36	±38	±29	±38	±98	±50	±18
Walker,	42	395	403	612	398	648	**673**	643	634	460	891
Walk	±12	±58	±24	±164	±165	±110	±94	±114	±132	±173	±82
Ball in cup,	312	338	769	913	861	914	948	933	**962**	926	746
Catch	±63	±196	±43	±53	±233	±20	±6	±16	±28	±31	±91
500k											
Finger,	179	914	926	938	924	**974**	937	973	906	963	811
Spin	±166	±107	±45	±103	±132	±6	±41	±31	±152	±40	±46
Cartpole,	419	730	841	868	870	869	869	872	**975**	865	835
Swingup	±40	±152	±45	±10	±12	±9	±4	±5	±38	±11	±22
Reacher,	145	601	929	942	925	941	957	957	**973**	942	746
Easy	±30	±135	±44	±71	±79	±48	±16	±41	±36	±66	±25
Cheetah,	197	544	518	660	716	588	656	674	552	**719**	616
Run	±15	±50	±28	±96	±47	±22	±43	±37	±130	±51	±18
Walker,	42	858	902	921	916	936	**943**	939	929	928	891
Walk	±12	±82	±43	±45	±75	±23	±17	±10	±68	±30	±82
Ball in cup,	312	810	959	863	963	961	970	964	**979**	967	746
Catch	±63	±121	±27	±9	±8	±9	±4	±14	±17	±5	±91

5.3 Zero-Shot Generalization Evaluation

In this subsection, we report the studies conducted on two benchmarks representing two different types of generalization: Procgen [144] for level generalization in arcade games, and DMControl-GB [53] for vision generalization in robot control tasks.

5.3.1 Level Generalization on Procgen

In Table 3, the results of RAD [12] and DrAC [54] are based on their most suitable augmentation types for different environments, and UCB-DrAC selects the most suitable type of DA as a multi-armed bandit problem. Based on the comparison of RAD [12] and its underlying PPO algorithm [3], it is evident that appropriate augmentations are beneficial in almost every environment. Additionally, explicitly regularizing the policy and value functions after performing augmentations (as in DrAC [54]) leads to further improvements. The outstanding results of CLOP [111] and DRIBO [29] highlight the remarkable potential of subtly designed representation learning methods to distinguish task-relevant information from task-irrelevant information.

Table 3: **Evaluation of Generalization Ability on Procgen.** Agents are trained on the first 200 levels of each game and evaluated on unseen levels. The scores are copied from the original papers on UCB-DrAC [54] and DRIBO [29]. The mean and standard deviation values are calculated with 10 random seeds.

Game	PPO [3]	RandFM [97]	MixReg [49]	RAD [12]	DrAC [54]	UCB-DrAC [54]	CLOP [111]	DRIBO [29]
BigFish	4.0±1.2	0.6±0.8	7.1±1.6	9.9±1.7	8.7±1.4	9.7±1.0	**19.2±4.6**	10.9±1.6
StarPilot	24.7±3.4	8.8±0.7	32.4±1.5	33.4±5.1	29.5±5.4	30.2±2.8	**40.9±1.7**	36.5±3.0
FruitBot	26.7±0.8	24.5±0.7	27.3±0.8	27.3±1.8	28.2±0.8	28.3±0.9	29.8±0.3	**30.8±0.8**
BossFight	7.7±1.0	1.7±0.9	8.2±0.7	7.9±0.6	7.5±0.8	8.3±0.8	9.7±0.1	**12.0±0.5**
Ninja	5.9±0.7	6.1±0.8	6.8±0.5	6.9±0.8	7.0±0.4	6.9±0.6	5.8±0.4	**9.7±0.7**
Plunder	5.0±0.5	3.0±0.6	5.9±0.5	8.5±1.2	**9.5±1.0**	8.9±1.0	5.4±0.7	5.8±1.0
CaveFlyer	5.1±0.9	5.4±0.8	6.1±0.6	5.1±0.6	6.3±0.8	5.3±0.9	5.0±0.3	**7.5±1.0**
CoinRun	8.5±0.5	9.3±1.4	8.6±0.3	9.0±0.8	8.8±0.2	8.5±0.6	**9.6±0.1**	9.2±0.7
Jumper	5.8±0.5	5.3±0.6	6.0±0.3	6.5±0.6	6.6±0.4	6.4±0.6	5.6±0.2	**8.4±1.6**
Chaser	5.0±0.8	1.4±0.7	5.8±1.1	5.9±1.0	5.7±0.6	6.7±0.6	**8.7±0.2**	4.8±0.8
Climber	5.7±0.8	5.3±0.7	6.9±0.7	6.9±0.8	7.1±0.7	6.5±0.8	7.4±0.3	**8.1±1.6**
DodgeBall	**11.7±0.3**	0.5±0.4	1.7±0.4	2.8±0.7	4.3±0.8	4.7±0.7	7.2±1.2	3.8±0.9
Heist	2.4±0.5	2.4±0.6	2.6±0.4	4.1±1.0	4.0±0.8	4.0±0.7	4.5±0.2	**7.7±1.6**
Leaper	4.9±0.7	6.2±0.5	5.3±1.1	4.3±1.0	5.3±1.1	5.0±0.3	**9.2±0.2**	5.3±1.5
Maze	5.7±0.6	8.0±0.7	5.2±0.5	6.1±1.0	6.6±0.8	6.3±0.6	5.9±0.2	**8.5±1.6**
Miner	8.5±0.5	7.7±0.6	9.4±0.4	9.4±1.2	**9.8±0.6**	9.7±0.7	**9.8±0.3**	**9.8±0.9**

Table 4 shows the best augmentation type for each game (copied from the original paper of DrAC [54]). Random cropping achieves the best performance on 9 out of 16 instances, while 5 out of 16 game environments benefit significantly from photometric transformations, including

color jitter and random convolution. For a detailed understanding of the connection between the properties of environments and augmentation types, Figure 21 suggests that the visual differences between the training environment and the test environment act as a major factor when determining the best augmentation type. For example, the background styles of Climber vary significantly across different levels, and manipulating the color and other photometric factors is intuitively beneficial to generalization.

By contrast, the different levels of the maze game Chaser share similar visual information but exhibit increasing difficulty. Consequently, applying photometric augmentations is likely to fail in this setting, which is consistent with the experimental results. In such cases, the appropriate augmentation type is usually random cropping, which is beneficial to sample efficiency and contributes to improving the generalization performance. In addition, CaveFlyer is uniquely friendly with the rotation augmentation, which is often destructive in other games. A closer check of the game shows that the major regions of the observations (except the gray areas) feature different positions and angles, and rotation can effectively narrow down the differences among them.

Table 4: **Best augmentation types for DrAC [54] in different games.** The original experiments [54] investigate a set of eight transformations: cropping, grayscale, Cutout, Cutout-Color, flipping, rotation, random convolution and color jitter (all of them are shown in Figure 8).

Game	BigFish	StarPilot	FruitBot	BossFight	Ninja	Plunder	**CaveFlyer**	CoinRun
Aug Type	Crop	Crop	Crop	Flip	Color Jitter	Crop	**Rotate**	Random Conv
Game	Jumper	**Chaser**	**Climber**	DodgeBall	Heist	Leaper	Maze	Miner
Aug Type	Random Conv	**Crop**	**Color Jitter**	Crop	Crop	Crop	Crop	Color Jitter
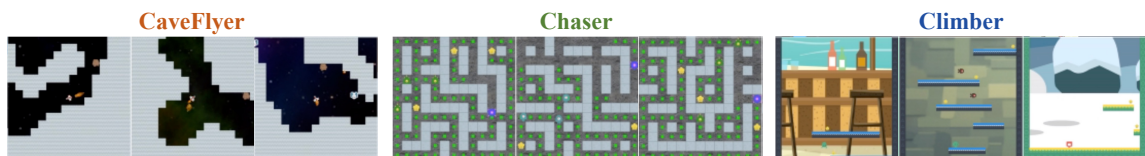
Figure 21: **Examples of three different game structures.** As shown in Table 4, the most effective DA for Climber, CaveFlyer, and Chaser are color jitter, rotation, and cropping, respectively.

5.3.2 Vision Generalization on DMControl-GB

As a variant of the DeepMind control suite [10], DMControl-GB [53] aims to evaluate the generalization ability of an agent by changing the image color or replacing the background with another image set (Figure 20). A comparison of performance levels achieved in seen environments (Table 2) and unseen environments (Table 5) shows that although DrQ [13] is prominent in terms of sample efficiency, the diversity derived from the naive application of cropping is limited, and a significant generalization gap is induced when this approach is transferred to unseen environments. To provide sufficient visual diversity for generalization, it is necessary to use strong augmentations such as random convolution and overlay, as indicated by the results of follow-up studies.

SVEA [15] and TLDA [87] both significantly outperform DrQ [13] by focusing on stabilizing the training process when leveraging strong augmentation to optimize the representation and

Table 5: **Evaluation of Generalization Ability on DMControl-GB.** The scores (means and standard deviations) are obtained by conducting training in a fixed environment and performing evaluations in two unseen test environments with random colors (top) and natural video backgrounds (bottom).

DMControl-GB (Random Colors)	SAC [17]	CURL [26]	RAD [12]	PAD [174]	DrQ [13]	SVEA [15]	SODA [53]	SIM [150]	TLDA [87]	SECANT [48]	PIE-G [42]
Walker, Stand	365 ±79	662 ±54	644 ±88	797 ±46	770 ±71	942 ±26	930 ±12	940 ±2	**947** ±26	939 ±7	941 ±35
Walker, Walk	144 ±19	445 ±99	400 ±61	468 ±47	520 ±91	760 ±145	697 ±66	803 ±33	823 ±58	856 ±31	**884** ±20
Cartpole, Swingup	248 ±24	454 ±110	590 ±53	837 ±63	630 ±52	837 ±23	831 ±21	841 ±13	760 ±60	**866** ±15	749 ±46
Ball in cup, Catch	151 ±36	231 ±92	541 ±29	563 ±50	365 ±210	**961** ±7	949 ±19	953 ±7	932 ±32	958 ±7	**964** ±7
Finger, Spin	504 ±114	691 ±12	667 ±154	803 ±72	776 ±134	**977** ±5	793 ±128	960 ±6	—	910 ±115	—
Cheetah, Run	133 ±26	—	—	159 ±28	100 ±27	273 ±23	294 ±34	—	371 ±51	**582** ±64	364 ±40
(Natural Videos)											
Walker, Stand	274 ±39	852 ±75	745 ±146	935 ±20	873 ±83	961 ±8	955 ±13	963 ±5	**973** ±6	932 ±15	957 ±12
Walker, Walk	104 ±14	556 ±133	606 ±63	717 ±79	682 ±89	819 ±71	768 ±38	861 ±33	**873** ±34	842 ±47	**870** ±22
Cartpole, Swingup	204 ±20	404 ±67	373 ±72	521 ±76	485 ±105	**782** ±27	758 ±62	770 ±13	671 ±57	752 ±38	597 ±61
Ball in cup, Catch	172 ±46	316 ±119	481 ±26	436 ±55	318 ±157	871 ±106	875 ±56	820 ±135	887 ±58	903 ±49	**922** ±20
Finger, Spin	276 ±81	502 ±19	400 ±64	691 ±80	533 ±119	808 ±33	695 ±94	81 ±38	—	**861** ±102	837 ±107
Cheetah, Run	80 ±19	—	—	206 ±34	102 ±30	292 ±32	229 ±29	—	356 ±52	**428** ±70	287 ±20

policy together. Another way to improve generalization is to decouple the unsupervised representation learning and the RL optimization process, either in an iterative manner (e.g., SODA [53] and SIM [150]) or in a sequential manner (e.g., SECANT [48]). Moreover, pre-trained encoders from off-the-shelf image datasets such as PIE-G [42] from ImageNet [80] also show attractive potential to provide generalizable representations in downstream tasks.

6   Discussion and Future Works

DA techniques have substantially improved the sample efficiency and generalization abilities of visual RL methods; however, many challenges remain to be addressed. In this section, we elaborate on these points and highlight key directions for future research, encompassing the opportunities, limitations, and underlying mechanisms of leveraging DA in visual RL.

6.1   Towards Semantic-Level DA

It can be considered as a kind of feature manipulation technique that alters the relative contributions of task-relevant and task-irrelevant features in the gradient update steps of the utilized network [90]. In this context, an ideal (albeit theoretical) DA method would operate at the semantic level, possessing the capability to precisely identify features pertinent to the current label or task while effectively perturbing irrelevant information.

However, this assumption underlying label-preserving transformations in SL and optimality-invariant transformations in RL proves challenging to uphold in practice, particularly when implementing pixel-level augmentations. The fundamental limitation of pixel-level approaches becomes evident when considering their mechanism: such augmentations, which aim to transform each pixel in a context-agnostic manner, inherently struggle to discriminate between task-relevant and task-irrelevant information [87]. This indiscriminate modification of pixels often results in the inadvertent alteration of critical task-relevant features, thereby compromising the efficacy of DA techniques, particularly in the domain of visual RL. Therefore, a promising avenue for advancing DA techniques lies in the development of semantic-level augmentation strategies. These strategies offer a more sophisticated approach compared to conventional pixel-level manipulations.

Several recent studies have attempted to move towards semantic-level DA by focusing on preserving task-relevant information. For example, EXPAND [122] and TLDA [87], as discussed in Section 3.5, propose methods to prevent augmentation of salient or sensitive areas in observed images, thereby maintaining critical visual information. In the broader computer vision community, KeepAugment [123] uses a saliency map to identify the key regions and then preserves these informative regions during augmentation to produce reliable training samples. While not directly a DA technique, VAI [5] employs unsupervised keypoint detection and visual attention mechanisms, combined with a reconstruction loss, to compel the encoder to embed only the foreground information of the input image. This method effectively introduces an inductive bias based on the assumption that key information controlling the objective in observations typically resides in the foreground, thereby prioritizing task-relevant features.

Recent advancements in pre-trained generative models have opened new avenues for achieving semantic-level augmentation [132]. The robust generative capabilities of large multi-modal models offer a promising DA approach that can be controlled through prompts. For instance, these models can be instructed to "replace the background of a robotic arm with an outdoor scene while keeping the arm itself unchanged". Such prompt-driven DA transformations have the potential to generate diverse augmented data while retaining semantic invariance. The application of generative augmentation in visual RL is still in its nascent stages. This emerging field presents a fertile ground for further exploration, particularly in developing methods that can leverage the semantic understanding of these models to produce task-relevant augmentations. Future research could fo-

cus on optimizing prompt engineering for RL-specific tasks, investigating the impact of generated data on policy learning, and developing techniques to ensure the generated augmentations align with the underlying dynamics of the RL environment.

6.2 Trade-off between Training Stability and Generalization

In practice, DrQ [13, 14] and RAD [12] that leverage weak DA such as random cropping as implicit regularization methods can yield significantly improved sample efficiency during training, while a noticeable generalization gap is observed when these approaches are transferred to unseen environments [53, 15, 48]. Furthermore, more diverse augmentations, such as color jitter, have the potential to improve generalization but tend to result in unstable optimization and poor sample efficiency [12, 15]. Therefore, a dilemma of balancing between stability and generalization is persistent when applying DA in visual RL. This challenge is particularly acute due to the inherently fragile nature of the optimization process in RL [48].

This dilemma is frequently attributed to the conflation of policy optimization and representation learning in current end-to-end visual RL algorithms [48, 53]. Consequently, a logical approach is to decouple these processes, independently learning a robust representation and a competent policy, as elaborated in Section 4.3 and Section 4.4. Such decoupling facilitates the application of heavy augmentations to improve generalization while simultaneously employing weak augmentations to maintain satisfactory sample efficiency [53, 48]. This strategy effectively addresses the stability-generalization trade-off. Moreover, the dilemma is exacerbated by the limitations of pixel-level augmentation techniques. These methods, when applied intensively, risk inadvertently destroying critical features, further complicating the balance between effective augmentation and preservation of essential information.

Further insight into this dilemma can be gained through the lens of the bias-variance trade-off, a fundamental principle in machine learning [175]. Contemporary complex models, such as DNNs, typically exhibit low bias but high variance. Consequently, these models are prone to overfitting the training data, resulting in sub-optimal performance on unseen data. DA addresses this issue by introducing increased diversity, thereby reducing variance and enhancing the model's generalization capabilities [16]. Although DA may mitigate the issue of overfitting, certain augmentation combinations can actually lead to underfitting, making the training process unstable and challenging [89, 139]. Note that the issue of underfitting is more detrimental in RL, as its optimization process is more unstable than those of supervised tasks.

Overall, there are two potential paths to further balance training stability and generalization. Firstly, designing more effective augmented data generation methods to avoid corrupting task-relevant information, as discussed in Section 6.1. Secondly, optimizing existing paradigms for leveraging DA, such as decoupling policy optimization and representation learning.

6.3 Underlying Mechanisms of DA Efficacy in Visual RL

Given the widespread application and powerful impact of DA in visual RL, understanding its underlying mechanisms has become crucial. However, most works have simply employed DA as a basic component without delving deeper into 'why DA works' [13, 12, 14]. To gain a comprehensive understanding of DA's effectiveness in visual RL, this section begins by briefly reviewing

existing studies on the underlying mechanisms of DA within the broader context of deep learning (Section 6.3.1). Subsequently, we will explore in depth the unique mechanisms of DA's efficacy in visual RL tasks in Section 6.3.2.

6.3.1 Prevailing Perspectives on DA Effectiveness in DL

In recent years, numerous efforts have been made to investigate the theoretical guarantees for DA from various perspectives. These guarantees provide researchers with valuable insights into the practical effects of such approaches [89, 90, 176]. This section offers a concise overview of previous works on the theoretical foundations of DA, categorizing them into three main perspectives: implicit regularization [139, 176, 86], invariance learning [89, 177] and feature manipulation [90, 178].

Implicit Regularization vs. Explicit Regularization. Regularization is a fundamental technique in deep learning that aims to prevent overfitting and improve generalization abilities by constraining the complexity of a model [139, 179, 111]. The regularization strategies of DA act on the training data instead of the model's parameters and hence can be considered a type of implicit regularization approach instead of an explicit regularization technique that imposes constraints on the parameters, such as minimizing the $\mathcal{L}_2$ norms of the parameters [176]. By keeping the parameter space intact, this data-driven regularization approach can maintain the model's representational capacity while increasing its robustness [13, 86]. In fact, DA is more straightforward than explicit regularization that integrates the prior knowledge into objective functions, and neural networks can implicitly encode the attributes of DA without explicitly training towards these objectives [180–182]. Furthermore, attempts have also been made to derive explicit regularizers to describe the implicit regularization effect of DA [140, 183].

Transformation Invariance. Invariance is an essential property of all intelligent systems that makes them generalize effectively [184]. The purpose of DA is to constrain a model's output to be invariant when applying task-irrelevant transformations to the input data [100, 54]. It has been widely accepted that translation invariance is an inherent feature of CNNs [180], whereas other types of transformation invariance, such as rotation invariance, must be induced by corresponding augmentations [88]. The definition of DA assumes that semantics are invariant to data transformation [51, 13], which implies that performing optimization with augmentation can result in implicit invariances. Furthermore, the specific details of augmentations can be used to encode prior knowledge about task-specific or dataset-specific invariances [184].

Feature Manipulation. An alternative explanation of how DA works is derived from the perspective of feature manipulation [185–187]. Learning meaningful features from high-dimensional data is empirically challenging, as critical features are often highly sparse and associated with spurious features such as dense noise. In practice, this may result in the network's overfitting the noisy features instead of properly learning the critical features [188]. First, by adjusting the relative contributions of the original data features, DA can effectively facilitate the incorporation of informative but hard-to-learn features into the learning process [90]. Second, the latest research shows that leveraging DA in contrastive learning can decouple spurious features from the representations of positive samples. By ignoring the decoupled features, the performance of networks may be boosted by focusing on the learning of resistant features [178].

6.3.2 Specialized Mechanisms of DA in Visual RL

The underlying mechanisms of DA in visual RL partially align with those observed in other domains, as discussed in Section 6.3.1. For instance, applying random shift to input observations without modifying other algorithmic details can be viewed as a form of implicit regularization [135, 183]. Additionally, the improvements in visual generalization achieved through DA can be attributed to the previously mentioned concepts of transform invariance and feature manipulation [55]. However, several remarkable phenomena unique to applying DA in visual RL cannot be adequately explained by mechanisms from other domains.

As illustrated by the blue training curve in Figure 22, visual RL agents (based on the DDPG algorithm [4] in this example) fail to achieve an effective decision policy in the classic continuous control task *Walker Run* from the DeepMind Control suite [10]. Remarkably, merely applying simple random shift transformations to input observations, without any other modifications to the algorithm, results in superior performance [14], as demonstrated by the orange curve in Figure 22. This striking improvement in training efficiency for visual RL stands in stark contrast to the incremental performance gains typically observed when applying DA in other task domains [91]. Such a significant disparity suggests that previous understandings of DA's mechanisms are insufficient to fully explain its role in visual RL tasks. Instead, this remarkable enhancement implies that DA must effectively overcome some critical bottleneck unique to visual RL that previously limited its training efficacy. This

Figure 22: Unlike in tasks from other domains, DA decisively enhances the training efficiency of visual RL.

phenomenon underscores the need for a deeper investigation into the specific mechanisms by which DA contributes to the success of visual RL algorithms.
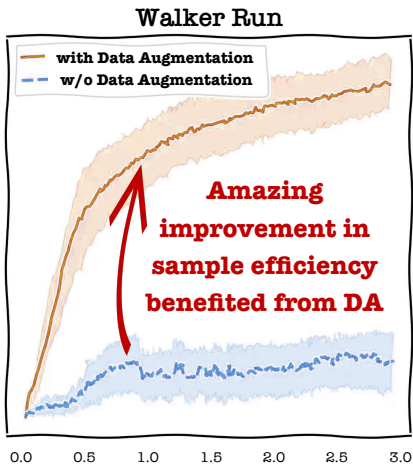
The most recent investigation [136] has unveiled that DA's remarkable effectiveness in visual RL stems from its ability to mitigate the **plasticity loss** of deep neural networks. Plasticity, referring to the capacity of deep neural networks to continually learn from new data, gradually diminishes during training with non-stationary objectives [189, 190]. The inherent nature of DRL necessitates that agents continuously refine their policies through environmental interactions, resulting in intrinsically non-stationary data streams and optimization objectives [191]. This characteristic of DRL paradigms renders plasticity loss a critical impediment to achieving sample-efficient applications, as the networks must maintain their adaptability throughout the learning process [192, 193]. Compared to traditional state-based RL tasks, visual RL algorithms suffer from more severe plasticity loss due to increased task complexity and larger network architectures. It has been demonstrated through ingenious experiments [136] that without DA, agents fail to train effectively due to catastrophic plasticity loss, while applying DA significantly alleviates this bottleneck. Furthermore, DA's efficacy in mitigating plasticity loss surpasses that of several interventions specifically designed for this purpose, such as Layer Normalization [194], Shrink & Perturb [195], and CReLU [196].

6.4 Unique Characteristics of DA in Visual RL versus Other Domains

Given the widespread application of DA across various domains in deep learning [100, 197], a pertinent question naturally arises:

Does the implementation of DA in visual RL exhibit significant distinctions from its utilization in other domains, particularly in supervised and unsupervised vision tasks?

Indeed, there are substantial differences, which underscores the necessity of organizing a survey specifically focused on DA in visual RL. This section will delineate the most salient differences in DA implementation between visual RL and other domains. Further exploration of these distinctions and the development of tailored DA techniques for the visual RL scenario represent crucial directions for future research.

Diverse Augmentable Data Types. Compared to typical supervised or unsupervised vision tasks, RL data is inherently more complex. On one hand, RL data encompasses three distinct elements: state, action, and reward. On the other hand, RL involves long sequences of sequential decision-making data, known as trajectories. This complexity in data types enables a more diverse and flexible approach to transforming different data components in visual RL tasks. As introduced in Section 3, when categorizing based on the type of data being augmented, visual RL incorporates at least three classes of augmentation: observation augmentation, transition augmentation, and trajectory augmentation. While existing works predominantly employ the simplest and most direct approach of observation augmentation [12, 14], the advancement of generative models such as diffusion techniques is likely to precipitate the emergence of more sophisticated yet diverse DA techniques in visual RL scenarios [134, 130]. This trend towards more complex augmentation strategies promises to exploit the rich structure of RL data more fully, potentially leading to significant improvements in sample efficiency and generalization capabilities.

Distinctive Implementation Details. Due to the nonstationary nature of RL, there are significant differences in the optimal practices for applying DA in visual RL compared to other scenarios. Firstly, contrary to supervised vision tasks such as image classification, where heavy transformations like Mixup [100] and CutMix [103] demonstrate notable advantages over traditional image transformations, in visual RL, random cropping has emerged as the most practical augmentation technique [12, 54]. Consequently, the approach to harnessing augmented data must be thoughtfully designed to avoid potential destabilization of the optimization process while effectively exploiting the generalization capabilities induced by DA [87, 135]. Secondly, the timing of augmentation application is critical in RL [198], in contrast to supervised learning tasks [199], due to the heightened time sensitivity of augmentation in RL contexts. For example, optimality-invariant augmentations such as cropping should be implemented as early as possible to enhance sample efficiency and expedite the RL training process. Conversely, prior-based strong augmentations like color jitter may interfere with RL training, suggesting that these techniques might be more effectively employed after RL optimization for knowledge distillation [198].

Unique Underlying Mechanisms. As discussed in Section 6.3.2, contrary to the general understanding of DA's mechanisms, it has been discovered that DA effectively addresses a bottleneck

unique to RL: plasticity loss [136]. This insight explains the remarkable extent to which DA enhances the sample efficiency of visual RL algorithms [14]. The distinctive mechanism through which DA operates in this context necessitates a paradigm shift in our approach to designing DA methods for visual RL. Specifically, future work must adopt a novel perspective in approaching DA for visual RL by focusing on mitigating plasticity loss, a consideration that has been largely overlooked in traditional DA approaches. This shift in focus represents a significant departure from conventional DA strategies and opens up new avenues for research in visual RL.

6.5 The Role of Visual RL and DA in the Age of Foundation Models

In recent years, foundation models, particularly large language models, have emerged rapidly, showcasing extraordinary intelligence and driving a new wave of AI innovation [200, 201]. In this era of large foundation models, we must consider two key questions:

Does the classic RL paradigm, as represented by visual RL, still retain research value and necessity?

Additionally, what role does DA play in this evolving landscape?

Clarifying the roles of visual RL and DA in the Age of Foundation Models is important for two reasons. First, it ensures that this survey's content remains pertinent and valuable in the current AI landscape. Second, it offers meaningful guidance for the future development of visual RL and DA. This section will address these two questions systematically.

Primarily, the classic RL paradigm, exemplified by visual RL, remains an indispensable component in achieving super-human decision-making intelligence. Currently, there are two primary approaches to leveraging foundation models in decision-making tasks.

- The first approach leverages pre-trained multi-modal large models for high-level perception and planning, harnessing their comprehensive understanding and reasoning capabilities to enhance strategic decision-making in complex environments [202–204]. In this context, RL remains crucial for training the low-level control policy. This policy generates specific actions based on task-relevant features extracted by foundation models, enabling effective agent-environment interaction [205, 206]. Consequently, RL bridges the gap between the high-level perception and planning capabilities of foundation models and the concrete action execution required in real-world scenarios.

- The second category of methods adopts the pre-training paradigm for data-driven offline policy training [207–209], drawing inspiration from the success of foundation models in other domains. In this paradigm, offline pre-training can be viewed as seeking an optimal initialization for online RL, while online fine-tuning is imperative for achieving high-level decision-making intelligence [210, 211]. This approach addresses two critical aspects. Firstly, due to the inherent distribution shift between offline data and real-world scenarios, online RL is necessary to correct these biases [212]. Secondly, only through exploration in online learning can the agent transcend the limitations of human-collected offline data and potentially surpass human-level intelligence [213, 214].

Furthermore, DA will undoubtedly continue to play a crucial role in visual RL and other RL tasks that utilize high-dimensional features as input. Primarily, DA remains a direct and effective

method for expanding datasets and incorporating human prior knowledge [134, 130]. In decision-making tasks such as robotic control, the availability of training data is significantly more limited compared to language and vision tasks. Consequently, designing more powerful DA techniques is essential for training large decision models. Moreover, as discussed in Section 6.3.2, DA effectively mitigates plasticity loss during online RL training. Without DA, even when employing pre-trained visual encoders for feature extraction, visual RL algorithms would still suffer from catastrophic plasticity loss, impeding efficient training [42, 136]. As foundation models continue to evolve, RL is tasked with handling increasingly complex decision-making scenarios, and agents are required to possess continual fine-tuning capabilities. This evolution in the field underscores the critical need for agents to retain adaptive capabilities, emphasizing the continued relevance and importance of DA research and application.

6.6   Limitations of DA

While DA has demonstrated significant benefits in visual RL, as extensively discussed in the preceding sections, it is crucial to acknowledge its limitations and potential drawbacks to provide a comprehensive understanding of its applicability and effectiveness.

1. The applications of DA are highly task-specific and require extensive expert knowledge [54]. In practice, DA's effectiveness depends on prior knowledge of the variations between training and test environments, allowing for reliable specification of appropriate augmentation techniques [55]. For example, in DMControl-GB, only visual settings such as background colors are varied in the test environments, and specific DA techniques, such as random convolution, can effectively capture these prior variations [15, 48].

2. DA effectively mitigates plasticity loss in single-task visual RL, ensuring efficient training [136]. However, it proves insufficient for maintaining adequate plasticity in open-ended and continual RL scenarios, where significant plasticity degradation occurs over extended training periods despite its application [196, 215]. This limitation calls for more targeted interventions to maintain long-term plasticity in open-ended, multi-task RL, essential for developing adaptive foundational RL policies.

3. DA, which modifies observations after they are generated, provides versatile applicability without necessitating direct simulator manipulation [12]. This characteristic is particularly advantageous when the underlying simulation environment is inaccessible or unmodifiable. However, in scenarios where direct access to the simulator is available, domain randomization (DR) can generate more diverse and precise data [216, 217]. Consequently, in specific fields such as robot learning, DR may prove more effective than DA [60, 61].

4. Current DA techniques, primarily focused on image transformations of observations, are insufficient for generating truly diverse synthetic data. This limitation stems from their reliance on human-defined priors, which constrains the injection of novel, informative knowledge into the data [15]. However, the advent of increasingly powerful pre-trained generative models presents a promising avenue to overcome this bottleneck, potentially enabling DA to produce substantially richer training data [134].

7 Conclusion

In this paper, we present a comprehensive survey of DA in the paradigm of visual RL. We first propose the High-Dimensional Contextual Markov Decision Process (HCMDP) as a general framework, elucidating the motivations for DA in improving sample efficiency and generalization. The main body of this survey meticulously examines existing related works, structured around two central themes: how to augment data and how to effectively utilize the augmented data. Subsequently, experimental results from widely used benchmarks demonstrate the efficacy of these techniques in visual RL. This survey also provides a list of current challenges and potential directions for future studies. In the following, we present a few suggestions and insights that are intended to benefit the relevant communities.

1. Compact and robust representation is vital for acquiring *sample-efficient* and *generalizable* visual RL agents; therefore, it is necessary to apply appropriate representation learning strategies to tackle the specific challenges of visual RL (Section 2.2). As a data-driven technique, DA is an essential component of representation learning and has great potential to be further explored (Section 2.3).

2. To fully harness the potential of DA, two complementary aspects must be addressed: how to augment data (Section 3) and how to effectively leverage augmented data (Section 4). The key to further advancing these aspects lies in two critical objectives: achieving semantic-level DA (Section 6.1), and attaining an effective balance between training stability and generalization ability (Section 6.2).

3. Beyond the common benefits such as regularization and feature manipulation that DA provides across all deep learning scenarios, there exists a unique mechanism behind DA's significant enhancement of visual RL training efficiency: its ability to effectively mitigate plasticity loss. Overcoming this RL-specific bottleneck should be a focal point for future research, emphasizing the development of more targeted augmentation strategies and other interventions (Section 6.3).

4. The difference between RL and SL should be given special attention when applying DA in visual RL, including fragile optimization process, the interactive data acquisition process and its absence of ground-truth labels (Section 6.4).

5. Visual RL, as a representative paradigm for learning control policies from high-dimensional features, remains a crucial component in the current era of large foundation models. DA, as a key element in achieving efficient and generalizable visual RL, warrants continued in-depth investigation (Section 6.5).

Overall, this survey strives to provide the first unified and principled framework for the large body of thriving research on DA in visual RL. We expect it to serve as a valuable guide for researchers and practitioners, and stimulate more inspiration in this fascinating field.

References

[1] Vincent François-Lavet, Peter Henderson, Riashat Islam, Marc G Bellemare, Joelle Pineau, et al. An introduction to deep reinforcement learning. *Foundations and Trends® in Machine Learning*, 11(3-4): 219–354, 2018.

[2] Volodymyr Mnih, Koray Kavukcuoglu, David Silver, Andrei A Rusu, Joel Veness, Marc G Bellemare, Alex Graves, Martin Riedmiller, Andreas K Fidjeland, Georg Ostrovski, et al. Human-level control through deep reinforcement learning. *nature*, 518(7540):529–533, 2015.

[3] John Schulman, Filip Wolski, Prafulla Dhariwal, Alec Radford, and Oleg Klimov. Proximal policy optimization algorithms. *arXiv preprint arXiv:1707.06347*, 2017.

[4] Timothy P Lillicrap, Jonathan J Hunt, Alexander Pritzel, Nicolas Heess, Tom Erez, Yuval Tassa, David Silver, and Daan Wierstra. Continuous control with deep reinforcement learning. *arXiv preprint arXiv:1509.02971*, 2015.

[5] Xudong Wang, Long Lian, and Stella X. Yu. Unsupervised visual attention and invariance for reinforcement learning. In *Proceedings of the IEEE/CVF Conference on Computer Vision and Pattern Recognition (CVPR)*, pages 6677–6687, June 2021.

[6] Denis Yarats, Amy Zhang, Ilya Kostrikov, Brandon Amos, Joelle Pineau, and Rob Fergus. Improving sample efficiency in model-free reinforcement learning from images. In *Proceedings of the AAAI Conference on Artificial Intelligence*, volume 35, 2021.

[7] David Silver, Thomas Hubert, Julian Schrittwieser, Ioannis Antonoglou, Matthew Lai, Arthur Guez, Marc Lanctot, Laurent Sifre, Dharshan Kumaran, Thore Graepel, et al. A general reinforcement learning algorithm that masters chess, shogi, and go through self-play. *Science*, 362, 2018.

[8] B Ravi Kiran, Ibrahim Sobh, Victor Talpaert, Patrick Mannion, Ahmad A Al Sallab, Senthil Yogamani, and Patrick Pérez. Deep reinforcement learning for autonomous driving: A survey. *IEEE Transactions on Intelligent Transportation Systems*, 2021.

[9] Dmitry Kalashnikov, Alex Irpan, Peter Pastor, Julian Ibarz, Alexander Herzog, Eric Jang, Deirdre Quillen, Ethan Holly, Mrinal Kalakrishnan, Vincent Vanhoucke, et al. Scalable deep reinforcement learning for vision-based robotic manipulation. In *Conference on Robot Learning*. PMLR, 2018.

[10] Yuval Tassa, Yotam Doron, Alistair Muldal, Tom Erez, Yazhe Li, Diego de Las Casas, David Budden, Abbas Abdolmaleki, Josh Merel, Andrew Lefrancq, et al. Deepmind control suite. *arXiv preprint arXiv:1801.00690*, 2018.

[11] Alex X Lee, Anusha Nagabandi, Pieter Abbeel, and Sergey Levine. Stochastic latent actor-critic: Deep reinforcement learning with a latent variable model. *Advances in Neural Information Processing Systems*, 33:741–752, 2020.

[12] Misha Laskin, Kimin Lee, Adam Stooke, Lerrel Pinto, Pieter Abbeel, and Aravind Srinivas. Reinforcement learning with augmented data. *Advances in neural information processing systems*, 33: 19884–19895, 2020.

[13] Denis Yarats, Ilya Kostrikov, and Rob Fergus. Image augmentation is all you need: Regularizing deep reinforcement learning from pixels. In *International Conference on Learning Representations*, 2020.

[14] Denis Yarats, Rob Fergus, Alessandro Lazaric, and Lerrel Pinto. Mastering visual continuous control: Improved data-augmented reinforcement learning. In *International Conference on Learning Representations*, 2021.

[15] Nicklas Hansen, Hao Su, and Xiaolong Wang. Stabilizing deep q-learning with convnets and vision transformers under data augmentation. *Advances in Neural Information Processing Systems*, 34, 2021.

[16] Chiyuan Zhang, Oriol Vinyals, Remi Munos, and Samy Bengio. A study on overfitting in deep reinforcement learning. *arXiv preprint arXiv:1804.06893*, 2018.

[17] Tuomas Haarnoja, Aurick Zhou, Pieter Abbeel, and Sergey Levine. Soft actor-critic: Off-policy maximum entropy deep reinforcement learning with a stochastic actor. In *International conference on machine learning*, pages 1861–1870. PMLR, 2018.

[18] Karl Cobbe, Oleg Klimov, Chris Hesse, Taehoon Kim, and John Schulman. Quantifying generalization in reinforcement learning. In *International Conference on Machine Learning*. PMLR, 2019.

[19] Zhuang Liu, Xuanlin Li, Bingyi Kang, and Trevor Darrell. Regularization matters in policy optimization-an empirical study on continuous control. In *International Conference on Learning Representations*, 2020.

[20] Matthew Hausknecht and Nolan Wagener. Consistent dropout for policy gradient reinforcement learning. *arXiv preprint arXiv:2202.11818*, 2022.

[21] Tao Yu, Zhizheng Zhang, Cuiling Lan, Zhibo Chen, and Yan Lu. Mask-based latent reconstruction for reinforcement learning. *arXiv preprint arXiv:2201.12096*, 2022.

[22] Kuang-Huei Lee, Ian Fischer, Anthony Liu, Yijie Guo, Honglak Lee, John Canny, and Sergio Guadarrama. Predictive information accelerates learning in rl. *Advances in Neural Information Processing Systems*, 33:11890–11901, 2020.

[23] Max Schwarzer, Ankesh Anand, Rishab Goel, R Devon Hjelm, Aaron Courville, and Philip Bachman. Data-efficient reinforcement learning with self-predictive representations. In *International Conference on Learning Representations*, 2020.

[24] Tao Yu, Cuiling Lan, Wenjun Zeng, Mingxiao Feng, Zhizheng Zhang, and Zhibo Chen. Playvirtual: Augmenting cycle-consistent virtual trajectories for reinforcement learning. *Advances in Neural Information Processing Systems*, 34, 2021.

[25] Tao Huang, Jiachen Wang, and Xiao Chen. Accelerating representation learning with view-consistent dynamics in data-efficient reinforcement learning. *arXiv preprint arXiv:2201.07016*, 2022.

[26] Michael Laskin, Aravind Srinivas, and Pieter Abbeel. Curl: Contrastive unsupervised representations for reinforcement learning. In *International Conference on Machine Learning*, pages 5639–5650. PMLR, 2020.

[27] Chenyu Sun, Hangwei Qian, and Chunyan Miao. Cclf: A contrastive-curiosity-driven learning framework for sample-efficient reinforcement learning. *arXiv preprint arXiv:2205.00943*, 2022.

[28] Minbeom Kim, Kyeongha Rho, Yong-duk Kim, and Kyomin Jung. Action-driven contrastive representation for reinforcement learning. *Plos one*, 17(3):e0265456, 2022.

[29] Jiameng Fan and Wenchao Li. Dribo: Robust deep reinforcement learning via multi-view information bottleneck. In *International Conference on Machine Learning*, pages 6074–6102. PMLR, 2022.

[30] Ankesh Anand, Evan Racah, Sherjil Ozair, Yoshua Bengio, Marc-Alexandre Côté, and R Devon Hjelm. Unsupervised state representation learning in atari. *Advances in neural information processing systems*, 2019.

[31] Thanh Nguyen, Tung M Luu, Thang Vu, and Chang D Yoo. Sample-efficient reinforcement learning representation learning with curiosity contrastive forward dynamics model. In *2021 IEEE/RSJ International Conference on Intelligent Robots and Systems (IROS)*, pages 3471–3477. IEEE, 2021.

[32] Jinhua Zhu, Yingce Xia, Lijun Wu, Jiajun Deng, Wengang Zhou, Tao Qin, Tie-Yan Liu, and Houqiang Li. Masked contrastive representation learning for reinforcement learning. *IEEE Transactions on Pattern Analysis and Machine Intelligence*, 2022.

[33] Bogdan Mazoure, Remi Tachet des Combes, Thang Long Doan, Philip Bachman, and R Devon Hjelm. Deep reinforcement and infomax learning. In *Advances in Neural Information Processing Systems*, 2020.

[34] Bang You, Oleg Arenz, Youping Chen, and Jan Peters. Integrating contrastive learning with dynamic models for reinforcement learning from images. *Neurocomputing*, 2022.

[35] Danijar Hafner, Timothy Lillicrap, Ian Fischer, Ruben Villegas, David Ha, Honglak Lee, and James Davidson. Learning latent dynamics for planning from pixels. In *International conference on machine learning*, pages 2555–2565. PMLR, 2019.

[36] Danijar Hafner, Timothy Lillicrap, Jimmy Ba, and Mohammad Norouzi. Dream to control: Learning behaviors by latent imagination. In *International Conference on Learning Representations*, 2019.

[37] Danijar Hafner, Timothy P Lillicrap, Mohammad Norouzi, and Jimmy Ba. Mastering atari with discrete world models. In *International Conference on Learning Representations*, 2020.

[38] Adam Stooke, Kimin Lee, Pieter Abbeel, and Michael Laskin. Decoupling representation learning from reinforcement learning. In *International Conference on Machine Learning*, pages 9870–9879. PMLR, 2021.

[39] Denis Yarats, Rob Fergus, Alessandro Lazaric, and Lerrel Pinto. Reinforcement learning with prototypical representations. In *International Conference on Machine Learning*. PMLR, 2021.

[40] Hao Liu and Pieter Abbeel. Behavior from the void: Unsupervised active pre-training. *Advances in Neural Information Processing Systems*, 34, 2021.

[41] Michael Laskin, Hao Liu, Xue Bin Peng, Denis Yarats, Aravind Rajeswaran, and Pieter Abbeel. Cic: Contrastive intrinsic control for unsupervised skill discovery. *arXiv preprint arXiv:2202.00161*, 2022.

[42] Zhecheng Yuan, Zhengrong Xue, Bo Yuan, Xueqian Wang, Yi Wu, Yang Gao, and Huazhe Xu. Pre-trained image encoder for generalizable visual reinforcement learning. In *First Workshop on Pre-training: Perspectives, Pitfalls, and Paths Forward at ICML 2022*, 2022.

[43] Che Wang, Xufang Luo, Keith Ross, and Dongsheng Li. Vrl3: A data-driven framework for visual deep reinforcement learning. *arXiv preprint arXiv:2202.10324*, 2022.

[44] Simone Parisi, Aravind Rajeswaran, Senthil Purushwalkam, and Abhinav Gupta. The unsurprising effectiveness of pre-trained vision models for control. In *International Conference on Machine Learning*, pages 17359–17371. PMLR, 2022.

[45] Tete Xiao, Ilija Radosavovic, Trevor Darrell, and Jitendra Malik. Masked visual pre-training for motor control. *arXiv preprint arXiv:2203.06173*, 2022.

[46] Rutav M Shah and Vikash Kumar. Rrl: Resnet as representation for reinforcement learning. In *International Conference on Machine Learning*, pages 9465–9476. PMLR, 2021.

[47] Kate Rakelly, Abhishek Gupta, Carlos Florensa, and Sergey Levine. Which mutual-information representation learning objectives are sufficient for control? *Advances in Neural Information Processing Systems*, 34:26345–26357, 2021.

[48] Linxi Fan, Guanzhi Wang, De-An Huang, Zhiding Yu, Li Fei-Fei, Yuke Zhu, and Animashree Anandkumar. Secant: Self-expert cloning for zero-shot generalization of visual policies. In *International Conference on Machine Learning*, 2021.

[49] Kaixin Wang, Bingyi Kang, Jie Shao, and Jiashi Feng. Improving generalization in reinforcement learning with mixture regularization. *Advances in Neural Information Processing Systems*, 2020.

[50] Weiran Huang, Mingyang Yi, and Xuyang Zhao. Towards the generalization of contrastive self-supervised learning. *arXiv preprint arXiv:2111.00743*, 2021.

[51] Connor Shorten and Taghi M Khoshgoftaar. A survey on image data augmentation for deep learning. *Journal of big data*, 6(1):1–48, 2019.

[52] Steven Y Feng, Varun Gangal, Jason Wei, Sarath Chandar, Soroush Vosoughi, Teruko Mitamura, and Eduard Hovy. A survey of data augmentation approaches for nlp. *arXiv preprint arXiv:2105.03075*, 2021.

[53] Nicklas Hansen and Xiaolong Wang. Generalization in reinforcement learning by soft data augmentation. In *2021 IEEE International Conference on Robotics and Automation (ICRA)*, pages 13611–13617. IEEE, 2021.

[54] Roberta Raileanu, Maxwell Goldstein, Denis Yarats, Ilya Kostrikov, and Rob Fergus. Automatic data augmentation for generalization in reinforcement learning. *Advances in Neural Information Processing Systems*, 34:5402–5415, 2021.

[55] Robert Kirk, Amy Zhang, Edward Grefenstette, and Tim Rocktäschel. A survey of generalisation in deep reinforcement learning. *arXiv preprint arXiv:2111.09794*, 2021.

[56] Xingyou Song, Yiding Jiang, Stephen Tu, Yilun Du, and Behnam Neyshabur. Observational overfitting in reinforcement learning. In *International Conference on Learning Representations*, 2019.

[57] Josh Tobin, Rachel Fong, Alex Ray, Jonas Schneider, Wojciech Zaremba, and Pieter Abbeel. Domain randomization for transferring deep neural networks from simulation to the real world. In *2017 IEEE/RSJ international conference on intelligent robots and systems (IROS)*. IEEE, 2017.

[58] Xue Bin Peng, Marcin Andrychowicz, Wojciech Zaremba, and Pieter Abbeel. Sim-to-real transfer of robotic control with dynamics randomization. In *2018 IEEE international conference on robotics and automation (ICRA)*, pages 3803–3810. IEEE, 2018.

[59] Fabio Muratore, Theo Gruner, Florian Wiese, Boris Belousov, Michael Gienger, and Jan Peters. Neural posterior domain randomization. In *Conference on Robot Learning*, pages 1532–1542. PMLR, 2022.

[60] Dániel Horváth, Gábor Erdős, Zoltán Istenes, Tomáš Horváth, and Sándor Földi. Object detection using sim2real domain randomization for robotic applications. *IEEE Transactions on Robotics*, 39(2): 1225–1243, 2022.

[61] Johann Huber, François Hélénon, Hippolyte Watrelot, Faïz Ben Amar, and Stéphane Doncieux. Domain randomization for sim2real transfer of automatically generated grasping datasets. In *2024 IEEE International Conference on Robotics and Automation (ICRA)*, pages 4112–4118. IEEE, 2024.

[62] Chaochao Lu, Biwei Huang, Ke Wang, José Miguel Hernández-Lobato, Kun Zhang, and Bernhard Schölkopf. Sample-efficient reinforcement learning via counterfactual-based data augmentation. *arXiv preprint arXiv:2012.09092*, 2020.

[63] Yijiong Lin, Jiancong Huang, Matthieu Zimmer, Yisheng Guan, Juan Rojas, and Paul Weng. Invariant transform experience replay: Data augmentation for deep reinforcement learning. *IEEE Robotics and Automation Letters*, 5(4):6615–6622, 2020.

[64] Max Schwarzer, Johan Samir Obando Ceron, Aaron Courville, Marc G Bellemare, Rishabh Agarwal, and Pablo Samuel Castro. Bigger, better, faster: Human-level atari with human-level efficiency. In *International Conference on Machine Learning*, pages 30365–30380. PMLR, 2023.

[65] Zhecheng Yuan, Tianming Wei, Shuiqi Cheng, Gu Zhang, Yuanpei Chen, and Huazhe Xu. Learning to manipulate anywhere: A visual generalizable framework for reinforcement learning. *arXiv preprint arXiv:2407.15815*, 2024.

[66] Simon Du, Akshay Krishnamurthy, Nan Jiang, Alekh Agarwal, Miroslav Dudik, and John Langford. Provably efficient rl with rich observations via latent state decoding. In *International Conference on Machine Learning*, pages 1665–1674. PMLR, 2019.

[67] Beining Han, Chongyi Zheng, Harris Chan, Keiran Paster, Michael Zhang, and Jimmy Ba. Learning domain invariant representations in goal-conditioned block mdps. *Advances in Neural Information Processing Systems*, 34, 2021.

[68] Dibya Ghosh, Jad Rahme, Aviral Kumar, Amy Zhang, Ryan P Adams, and Sergey Levine. Why generalization in rl is difficult: Epistemic pomdps and implicit partial observability. *Advances in Neural Information Processing Systems*, 34, 2021.

[69] Finale Doshi-Velez and George Konidaris. Hidden parameter markov decision processes: A semi-parametric regression approach for discovering latent task parametrizations. In *IJCAI: proceedings of the conference*, volume 2016, page 1432. NIH Public Access, 2016.

[70] Assaf Hallak, Dotan Di Castro, and Shie Mannor. Contextual markov decision processes. *arXiv preprint arXiv:1502.02259*, 2015.

[71] Manan Tomar, Utkarsh A Mishra, Amy Zhang, and Matthew E Taylor. Learning representations for pixel-based control: What matters and why? *arXiv preprint arXiv:2111.07775*, 2021.

[72] Yuke Zhu, Josiah Wong, Ajay Mandlekar, and Roberto Martín-Martín. robosuite: A modular simulation framework and benchmark for robot learning. *arXiv preprint arXiv:2009.12293*, 2020.

[73] Amy Zhang, Clare Lyle, Shagun Sodhani, Angelos Filos, Marta Kwiatkowska, Joelle Pineau, Yarin Gal, and Doina Precup. Invariant causal prediction for block mdps. In *International Conference on Machine Learning*, pages 11214–11224. PMLR, 2020.

[74] Shagun Sodhani, Franziska Meier, Joelle Pineau, and Amy Zhang. Block contextual mdps for continual learning. In *Learning for Dynamics and Control Conference*, pages 608–623. PMLR, 2022.

[75] Matthew Hausknecht and Peter Stone. Deep recurrent q-learning for partially observable mdps. In *2015 aaai fall symposium series*, 2015.

[76] Feiyang Pan, Tongzhe Zhang, Ling Luo, Jia He, and Shuoling Liu. Learn continuously, act discretely: Hybrid action-space reinforcement learning for optimal execution. In *Proceedings of the Thirty-First International Joint Conference on Artificial Intelligence (IJCAI-22)*, pages 3912–3918, 2022.

[77] Rui Yang, Jie Wang, Zijie Geng, Mingxuan Ye, Shuiwang Ji, Bin Li, and Feng Wu. Learning task-relevant representations for generalization via characteristic functions of reward sequence distributions. *arXiv preprint arXiv:2205.10218*, 2022.

[78] Yang Yu. Towards sample efficient reinforcement learning. In *IJCAI*, pages 5739–5743, 2018.

[79] Aaron van den Oord, Yazhe Li, and Oriol Vinyals. Representation learning with contrastive predictive coding. *arXiv preprint arXiv:1807.03748*, 2018.

[80] Jia Deng, Wei Dong, Richard Socher, Li-Jia Li, Kai Li, and Li Fei-Fei. Imagenet: A large-scale hierarchical image database. In *2009 IEEE conference on computer vision and pattern recognition*, pages 248–255. Ieee, 2009.

[81] Akshay Krishnamurthy, Alekh Agarwal, and John Langford. Pac reinforcement learning with rich observations. *Advances in Neural Information Processing Systems*, 29:1840–1848, 2016.

[82] Jesse Farebrother, Marlos C Machado, and Michael Bowling. Generalization and regularization in dqn. *arXiv preprint arXiv:1810.00123*, 2018.

[83] Maximilian Igl, Kamil Ciosek, Yingzhen Li, Sebastian Tschiatschek, Cheng Zhang, Sam Devlin, and Katja Hofmann. Generalization in reinforcement learning with selective noise injection and information bottleneck. *Advances in neural information processing systems*, 32, 2019.

[84] Amy Zhang, Rowan McAllister, Roberto Calandra, Yarin Gal, and Sergey Levine. Learning invariant representations for reinforcement learning without reconstruction. *arXiv preprint arXiv:2006.10742*, 2020.

[85] Mete Kemertas and Tristan Aumentado-Armstrong. Towards robust bisimulation metric learning. *Advances in Neural Information Processing Systems*, 34:4764–4777, 2021.

[86] Alex Hernández-García and Peter König. Data augmentation instead of explicit regularization. *arXiv preprint arXiv:1806.03852*, 2018.

[87] Zhecheng Yuan, Guozheng Ma, Yao Mu, Bo Xia, Bo Yuan, Xueqian Wang, Ping Luo, and Huazhe Xu. Don't touch what matters: Task-aware lipschitz data augmentationfor visual reinforcement learning. *arXiv preprint arXiv:2202.09982*, 2022.

[88] Alexander Immer, Tycho FA van der Ouderaa, Vincent Fortuin, Gunnar Rätsch, and Mark van der Wilk. Invariance learning in deep neural networks with differentiable laplace approximations. *arXiv preprint arXiv:2202.10638*, 2022.

[89] Aleksander Botev, Matthias Bauer, and Soham De. Regularising for invariance to data augmentation improves supervised learning. *arXiv preprint arXiv:2203.03304*, 2022.

[90] Ruoqi Shen, Sébastien Bubeck, and Suriya Gunasekar. Data augmentation as feature manipulation. In *International conference on machine learning*, pages 19773–19808. PMLR, 2022.

[91] Suorong Yang, Weikang Xiao, Mengcheng Zhang, Suhan Guo, Jian Zhao, and Furao Shen. Image data augmentation for deep learning: A survey. *arXiv preprint arXiv:2204.08610*, 2022.

[92] Terrance DeVries and Graham W Taylor. Improved regularization of convolutional neural networks with cutout. *arXiv preprint arXiv:1708.04552*, 2017.

[93] Nour Eldeen Khalifa, Mohamed Loey, and Seyedali Mirjalili. A comprehensive survey of recent trends in deep learning for digital images augmentation. *Artificial Intelligence Review*, pages 1–27, 2021.

[94] Simukayi Mutasa, Shawn Sun, and Richard Ha. Understanding artificial intelligence based radiology studies: What is overfitting? *Clinical imaging*, 65:96–99, 2020.

[95] Sebastien C Wong, Adam Gatt, Victor Stamatescu, and Mark D McDonnell. Understanding data augmentation for classification: when to warp? In *2016 international conference on digital image computing: techniques and applications (DICTA)*, pages 1–6. IEEE, 2016.

[96] Ekin D Cubuk, Barret Zoph, Dandelion Mane, Vijay Vasudevan, and Quoc V Le. Autoaugment: Learning augmentation strategies from data. In *Proceedings of the IEEE/CVF Conference on Computer Vision and Pattern Recognition*, pages 113–123, 2019.

[97] Kimin Lee, Kibok Lee, Jinwoo Shin, and Honglak Lee. Network randomization: A simple technique for generalization in deep reinforcement learning. *arXiv preprint arXiv:1910.05396*, 2019.

[98] Francisco J Moreno-Barea, Fiammetta Strazzera, José M Jerez, Daniel Urda, and Leonardo Franco. Forward noise adjustment scheme for data augmentation. In *2018 IEEE symposium series on computational intelligence (SSCI)*, pages 728–734. IEEE, 2018.

[99] Linjun Zhang, Zhun Deng, Kenji Kawaguchi, Amirata Ghorbani, and James Zou. How does mixup help with robustness and generalization? *arXiv preprint arXiv:2010.04819*, 2020.

[100] Hongyi Zhang, Moustapha Cisse, Yann N Dauphin, and David Lopez-Paz. mixup: Beyond empirical risk minimization. *arXiv preprint arXiv:1710.09412*, 2017.

[101] Tsung-Yi Lin, Michael Maire, Serge Belongie, James Hays, Pietro Perona, Deva Ramanan, Piotr Dollár, and C Lawrence Zitnick. Microsoft coco: Common objects in context. In *European conference on computer vision*, pages 740–755. Springer, 2014.

[102] Zhun Zhong, Liang Zheng, Guoliang Kang, Shaozi Li, and Yi Yang. Random erasing data augmentation. *arXiv preprint arXiv:1708.04896*, 2017.

[103] Sangdoo Yun, Dongyoon Han, Seong Joon Oh, Sanghyuk Chun, Junsuk Choe, and Youngjoon Yoo. Cutmix: Regularization strategy to train strong classifiers with localizable features. In *Proceedings of the IEEE/CVF international conference on computer vision*, pages 6023–6032, 2019.

[104] Terrance DeVries and Graham W Taylor. Dataset augmentation in feature space. *arXiv preprint arXiv:1702.05538*, 2017.

[105] Tsz-Him Cheung and Dit-Yan Yeung. Modals: Modality-agnostic automated data augmentation in the latent space. In *International Conference on Learning Representations*, 2020.

[106] Xiaofeng Liu, Yang Zou, Lingsheng Kong, Zhihui Diao, Junliang Yan, Jun Wang, Site Li, Ping Jia, and Jane You. Data augmentation via latent space interpolation for image classification. In *2018 24th International Conference on Pattern Recognition (ICPR)*, pages 728–733. IEEE, 2018.

[107] Hiroshi Ohno. Auto-encoder-based generative models for data augmentation on regression problems. *Soft Computing*, 24(11):7999–8009, 2020.

[108] Ashvin V Nair, Vitchyr Pong, Murtaza Dalal, Shikhar Bahl, Steven Lin, and Sergey Levine. Visual reinforcement learning with imagined goals. *Advances in neural information processing systems*, 31, 2018.

[109] Kaiyang Zhou, Yongxin Yang, Yu Qiao, and Tao Xiang. Domain generalization with mixstyle. In *International Conference on Learning Representations*, 2020.

[110] Xun Huang and Serge Belongie. Arbitrary style transfer in real-time with adaptive instance normalization. In *Proceedings of the IEEE international conference on computer vision*, pages 1501–1510, 2017.

[111] David Bertoin and Emmanuel Rachelson. Local feature swapping for generalization in reinforcement learning. *arXiv preprint arXiv:2204.06355*, 2022.

[112] Nadiia Chepurko, Ryan Marcus, Emanuel Zgraggen, Raul Castro Fernandez, Tim Kraska, and David Karger. Arda: automatic relational data augmentation for machine learning. *Proceedings of the VLDB Endowment*, 2020.

[113] Yonggang Li, Guosheng Hu, Yongtao Wang, Timothy Hospedales, Neil M Robertson, and Yongxin Yang. Differentiable automatic data augmentation. In *European Conference on Computer Vision*, pages 580–595. Springer, 2020.

[114] Peter Auer. Using confidence bounds for exploitation-exploration trade-offs. *Journal of Machine Learning Research*, 3(Nov):397–422, 2002.

[115] Yoonhee Gil, Jongchan Baek, Jonghyuk Park, and Soohee Han. Automatic data augmentation by upper confidence bounds for deep reinforcement learning. In *2021 21st International Conference on Control, Automation and Systems (ICCAS)*, pages 1199–1203. IEEE, 2021.

[116] Jane X Wang, Zeb Kurth-Nelson, Dhruva Tirumala, Hubert Soyer, Joel Z Leibo, Remi Munos, Charles Blundell, Dharshan Kumaran, and Matt Botvinick. Learning to reinforcement learn. *arXiv preprint arXiv:1611.05763*, 2016.

[117] Chelsea Finn, Pieter Abbeel, and Sergey Levine. Model-agnostic meta-learning for fast adaptation of deep networks. In *International conference on machine learning*, pages 1126–1135. PMLR, 2017.

[118] Chaoqi Chen, Jiongcheng Li, Xiaoguang Han, Xiaoqing Liu, and Yizhou Yu. Compound domain generalization via meta-knowledge encoding. In *2022 IEEE/CVF Conference on Computer Vision and Pattern Recognition (CVPR)*, pages 7109–7119, 2022. doi: 10.1109/CVPR52688.2022.00698.

[119] Samuel Greydanus, Anurag Koul, Jonathan Dodge, and Alan Fern. Visualizing and understanding atari agents. In *International conference on machine learning*, pages 1792–1801. PMLR, 2018.

[120] Alexander Mott, Daniel Zoran, Mike Chrzanowski, Daan Wierstra, and Danilo Jimenez Rezende. Towards interpretable reinforcement learning using attention augmented agents. *Advances in Neural Information Processing Systems*, 32, 2019.

[121] Ruohan Zhang, Faraz Torabi, Lin Guan, Dana H Ballard, and Peter Stone. Leveraging human guidance for deep reinforcement learning tasks. *arXiv preprint arXiv:1909.09906*, 2019.

[122] Lin Guan, Mudit Verma, Sihang Guo, Ruohan Zhang, and Subbarao Kambhampati. Widening the pipeline in human-guided reinforcement learning with explanation and context-aware data augmentation. *Advances in Neural Information Processing Systems*, 2021.

[123] Chengyue Gong, Dilin Wang, Meng Li, Vikas Chandra, and Qiang Liu. Keepaugment: A simple information-preserving data augmentation approach. In *Proceedings of the IEEE/CVF Conference on Computer Vision and Pattern Recognition*, pages 1055–1064, 2021.

[124] Jaehoon Choi, Taekyung Kim, and Changick Kim. Self-ensembling with gan-based data augmentation for domain adaptation in semantic segmentation. In *Proceedings of the IEEE/CVF International Conference on Computer Vision*, pages 6830–6840, 2019.

[125] Hadi Mansourifar, Lin Chen, and Weidong Shi. Virtual big data for gan based data augmentation. In *2019 IEEE International Conference on Big Data (Big Data)*, pages 1478–1487. IEEE, 2019.

[126] Xingyi Yang and Xinchao Wang. Diffusion model as representation learner. In *Proceedings of the IEEE/CVF International Conference on Computer Vision*, pages 18938–18949, 2023.

[127] Chenyu Zheng, Guoqiang Wu, and Chongxuan Li. Toward understanding generative data augmentation. *Advances in Neural Information Processing Systems*, 36, 2024.

[128] A Antoniou. Data augmentation generative adversarial networks. *arXiv preprint arXiv:1711.04340*, 2017.

[129] Baris Imre. An investigation of generative replay in deep reinforcement learning. B.S. thesis, University of Twente, 2021.

[130] Zhengbang Zhu, Hanye Zhao, Haoran He, Yichao Zhong, Shenyu Zhang, Yong Yu, and Weinan Zhang. Diffusion models for reinforcement learning: A survey. *arXiv preprint arXiv:2311.01223*, 2023.

[131] Tianhe Yu, Ted Xiao, Austin Stone, Jonathan Tompson, Anthony Brohan, Su Wang, Jaspiar Singh, Clayton Tan, Jodilyn Peralta, Brian Ichter, et al. Scaling robot learning with semantically imagined experience. *arXiv preprint arXiv:2302.11550*, 2023.

[132] Zoey Chen, Sho Kiami, Abhishek Gupta, and Vikash Kumar. Genaug: Retargeting behaviors to unseen situations via generative augmentation. *arXiv preprint arXiv:2302.06671*, 2023.

[133] Cong Lu, Philip Ball, Yee Whye Teh, and Jack Parker-Holder. Synthetic experience replay. *Advances in Neural Information Processing Systems*, 36, 2024.

[134] Haoran He, Chenjia Bai, Kang Xu, Zhuoran Yang, Weinan Zhang, Dong Wang, Bin Zhao, and Xuelong Li. Diffusion model is an effective planner and data synthesizer for multi-task reinforcement learning. *Advances in neural information processing systems*, 36, 2024.

[135] Guozheng Ma, Linrui Zhang, Haoyu Wang, Lu Li, Zilin Wang, Zhen Wang, Li Shen, Xueqian Wang, and Dacheng Tao. Learning better with less: Effective augmentation for sample-efficient visual reinforcement learning. *Advances in Neural Information Processing Systems*, 36, 2024.

[136] Guozheng Ma, Lu Li, Sen Zhang, Zixuan Liu, Zhen Wang, Yixin Chen, Li Shen, Xueqian Wang, and Dacheng Tao. Revisiting plasticity in visual reinforcement learning: Data, modules and training stages. In *The Twelfth International Conference on Learning Representations*, 2024. URL https://openreview.net/forum?id=0aR1s9YxoL.

[137] Abdulaziz Almuzairee, Nicklas Hansen, and Henrik I Christensen. A recipe for unbounded data augmentation in visual reinforcement learning. *arXiv preprint arXiv:2405.17416*, 2024.

[138] Michael Laskin, Denis Yarats, Hao Liu, Kimin Lee, Albert Zhan, Kevin Lu, Catherine Cang, Lerrel Pinto, and Pieter Abbeel. Urlb: Unsupervised reinforcement learning benchmark. *arXiv preprint arXiv:2110.15191*, 2021.

[139] Reza Moradi, Reza Berangi, and Behrouz Minaei. A survey of regularization strategies for deep models. *Artificial Intelligence Review*, 53(6):3947–3986, 2020.

[140] Randall Balestriero, Ishan Misra, and Yann LeCun. A data-augmentation is worth a thousand samples: Exact quantification from analytical augmented sample moments. *arXiv preprint arXiv:2202.08325*, 2022.

[141] Shuo Yang, Yijun Dong, Rachel Ward, Inderjit S Dhillon, Sujay Sanghavi, and Qi Lei. Sample efficiency of data augmentation consistency regularization. *arXiv preprint arXiv:2202.12230*, 2022.

[142] Junbo Zhang and Kaisheng Ma. Rethinking the augmentation module in contrastive learning: Learning hierarchical augmentation invariance with expanded views. In *Proceedings of the IEEE/CVF Conference on Computer Vision and Pattern Recognition*, 2022.

[143] Julius Von Kügelgen, Yash Sharma, Luigi Gresele, Wieland Brendel, Bernhard Schölkopf, Michel Besserve, and Francesco Locatello. Self-supervised learning with data augmentations provably isolates content from style. *Advances in Neural Information Processing Systems*, 34, 2021.

[144] Karl Cobbe, Chris Hesse, Jacob Hilton, and John Schulman. Leveraging procedural generation to benchmark reinforcement learning. In *International conference on machine learning*. PMLR, 2020.

[145] Tairan He, Yuge Zhang, Kan Ren, Che Wang, Weinan Zhang, Dongsheng Li, and Yuqing Yang. Aarl: Automated auxiliary loss for reinforcement learning. *openreview.net*, 2021.

[146] Marc Bellemare, Will Dabney, Robert Dadashi, Adrien Ali Taiga, Pablo Samuel Castro, Nicolas Le Roux, Dale Schuurmans, Tor Lattimore, and Clare Lyle. A geometric perspective on optimal representations for reinforcement learning. *Advances in neural information processing systems*, 32, 2019.

[147] Banafsheh Rafiee, Jun Jin, Jun Luo, and Adam White. What makes useful auxiliary tasks in reinforcement learning: investigating the effect of the target policy. *arXiv preprint arXiv:2204.00565*, 2022.

[148] Xiang Li, Jinghuan Shang, Srijan Das, and Michael S Ryoo. Does self-supervised learning really improve reinforcement learning from pixels? *arXiv preprint arXiv:2206.05266*, 2022.

[149] Tairan He, Yuge Zhang, Kan Ren, Minghuan Liu, Che Wang, Weinan Zhang, Yuqing Yang, and Dongsheng Li. Reinforcement learning with automated auxiliary loss search. *arXiv preprint arXiv:2210.06041*, 2022.

[150] Keyu Wu, Min Wu, Zhenghua Chen, Yuecong Xu, and Xiaoli Li. Generalizing reinforcement learning through fusing self-supervised learning into intrinsic motivation. *The 36th AAAI Conference on Artificial Intelligence (AAAI 2022)*, 2022.

[151] Michael Tschannen, Josip Djolonga, Paul K Rubenstein, Sylvain Gelly, and Mario Lucic. On mutual information maximization for representation learning. *arXiv preprint arXiv:1907.13625*, 2019.

[152] Marco Federici, Anjan Dutta, Patrick Forré, Nate Kushman, and Zeynep Akata. Learning robust representations via multi-view information bottleneck. *arXiv preprint arXiv:2002.07017*, 2020.

[153] Kaiming He, Haoqi Fan, Yuxin Wu, Saining Xie, and Ross Girshick. Momentum contrast for unsupervised visual representation learning. In *Proceedings of the IEEE/CVF Conference on Computer Vision and Pattern Recognition (CVPR)*, June 2020.

[154] Tianwei Ni, Benjamin Eysenbach, Erfan Seyedsalehi, Michel Ma, Clement Gehring, Aditya Mahajan, and Pierre-Luc Bacon. Bridging state and history representations: Understanding self-predictive rl. *arXiv preprint arXiv:2401.08898*, 2024.

[155] Minsong Liu, Yuanheng Zhu, Yaran Chen, and Dongbin Zhao. Enhancing reinforcement learning via transformer-based state predictive representations. *IEEE Transactions on Artificial Intelligence*, 2024.

[156] Dan Hendrycks, Norman Mu, Ekin D Cubuk, Barret Zoph, Justin Gilmer, and Balaji Lakshminarayanan. Augmix: A simple data processing method to improve robustness and uncertainty. *arXiv preprint arXiv:1912.02781*, 2019.

[157] Kaiming He, Xinlei Chen, Saining Xie, Yanghao Li, Piotr Dollár, and Ross Girshick. Masked autoencoders are scalable vision learners. *arXiv preprint arXiv:2111.06377*, 2021.

[158] Tom Brown, Benjamin Mann, Nick Ryder, Melanie Subbiah, Jared D Kaplan, Prafulla Dhariwal, Arvind Neelakantan, Pranav Shyam, Girish Sastry, Amanda Askell, et al. Language models are few-shot learners. *Advances in neural information processing systems*, 33:1877–1901, 2020.

[159] Zhen Wang, Liu Liu, Yiqun Duan, and Dacheng Tao. Sin: Semantic inference network for few-shot streaming label learning. *IEEE Transactions on Neural Networks and Learning Systems*, pages 1–14, 2022. doi: 10.1109/TNNLS.2022.3162747.

[160] Steven Hansen, Will Dabney, Andre Barreto, Tom Van de Wiele, David Warde-Farley, and Volodymyr Mnih. Fast task inference with variational intrinsic successor features. *arXiv preprint arXiv:1906.05030*, 2019.

[161] Hao Liu and Pieter Abbeel. Aps: Active pretraining with successor features. In *International Conference on Machine Learning*, pages 6736–6747. PMLR, 2021.

[162] Max Schwarzer, Nitarshan Rajkumar, Michael Noukhovitch, Ankesh Anand, Laurent Charlin, R Devon Hjelm, Philip Bachman, and Aaron C Courville. Pretraining representations for data-efficient reinforcement learning. *Advances in Neural Information Processing Systems*, 34, 2021.

[163] Nicklas Hansen, Zhecheng Yuan, Yanjie Ze, Tongzhou Mu, Aravind Rajeswaran, Hao Su, Huazhe Xu, and Xiaolong Wang. On pre-training for visuo-motor control: Revisiting a learning-from-scratch baseline. *arXiv preprint arXiv:2212.05749*, 2022.

[164] Suraj Nair, Aravind Rajeswaran, Vikash Kumar, Chelsea Finn, and Abhinav Gupta. R3m: A universal visual representation for robot manipulation. *arXiv preprint arXiv:2203.12601*, 2022.

[165] Lukasz Kaiser, Mohammad Babaeizadeh, Piotr Milos, Blazej Osinski, Roy H Campbell, Konrad Czechowski, Dumitru Erhan, Chelsea Finn, Piotr Kozakowski, Sergey Levine, et al. Model-based reinforcement learning for atari. *arXiv preprint arXiv:1903.00374*, 2019.

[166] Li Shen, Long Yang, Shixiang Chen, Bo Yuan, Xueqian Wang, Dacheng Tao, et al. Penalized proximal policy optimization for safe reinforcement learning. *arXiv preprint arXiv:2205.11814*, 2022.

[167] Charles Beattie, Joel Z Leibo, Denis Teplyashin, Tom Ward, Marcus Wainwright, Heinrich Küttler, Andrew Lefrancq, Simon Green, Víctor Valdés, Amir Sadik, et al. Deepmind lab. *arXiv preprint arXiv:1612.03801*, 2016.

[168] Austin Stone, Oscar Ramirez, Kurt Konolige, and Rico Jonschkowski. The distracting control suite–a challenging benchmark for reinforcement learning from pixels. *arXiv preprint arXiv:2101.02722*, 2021.

[169] Jake Grigsby and Yanjun Qi. Measuring visual generalization in continuous control from pixels. *arXiv preprint arXiv:2010.06740*, 2020.

[170] Amy Zhang, Yuxin Wu, and Joelle Pineau. Natural environment benchmarks for reinforcement learning. *arXiv preprint arXiv:1811.06032*, 2018.

[171] Lu Li, Jiafei Lyu, Guozheng Ma, Zilin Wang, Zhenjie Yang, Xiu Li, and Zhiheng Li. Normalization enhances generalization in visual reinforcement learning. In *Proceedings of the 23rd International Conference on Autonomous Agents and Multiagent Systems*, pages 1137–1146, 2024.

[172] Ziyu Wang, Tom Schaul, Matteo Hessel, Hado Hasselt, Marc Lanctot, and Nando Freitas. Dueling network architectures for deep reinforcement learning. In *International conference on machine learning*, pages 1995–2003. PMLR, 2016.

[173] Zhen Wang, Liu Liu, Yiqun Duan, Yajing Kong, and Dacheng Tao. Continual learning with life-long vision transformer. In *Proceedings of the IEEE/CVF Conference on Computer Vision and Pattern Recognition (CVPR)*, pages 171–181, June 2022.

[174] Nicklas Hansen, Rishabh Jangir, Yu Sun, Guillem Alenyà, Pieter Abbeel, Alexei A Efros, Lerrel Pinto, and Xiaolong Wang. Self-supervised policy adaptation during deployment. *arXiv preprint arXiv:2007.04309*, 2020.

[175] Tom Dietterich. Overfitting and undercomputing in machine learning. *ACM computing surveys (CSUR)*, 27(3):326–327, 1995.

[176] Randall Balestriero, Leon Bottou, and Yann LeCun. The effects of regularization and data augmentation are class dependent. *arXiv preprint arXiv:2204.03632*, 2022.

[177] Song Mei, Theodor Misiakiewicz, and Andrea Montanari. Learning with invariances in random features and kernel models. In *Conference on Learning Theory*, pages 3351–3418. PMLR, 2021.

[178] Zixin Wen and Yuanzhi Li. Toward understanding the feature learning process of self-supervised contrastive learning. In *International Conference on Machine Learning*. PMLR, 2021.

[179] Zhen Wang, Liu Liu, and Dacheng Tao. Deep streaming label learning. In *International Conference on Machine Learning (ICML)*, volume 119, pages 9963–9972, 2020.

[180] Eddie Yan and Yanping Huang. Do cnns encode data augmentations? In *2021 International Joint Conference on Neural Networks (IJCNN)*, pages 1–8. IEEE, 2021.

[181] inchao Wang Xingyi Yang. Neural metamorphosis. *ECCV*, 2024.

[182] Damien A Dablain and Nitesh V Chawla. Towards understanding how data augmentation works with imbalanced data. *arXiv preprint arXiv:2304.05895*, 2023.

[183] Jianshu Hu, Yunpeng Jiang, and Paul Weng. Revisiting data augmentation in deep reinforcement learning. In *The Twelfth International Conference on Learning Representations*, 2024. URL https://openreview.net/forum?id=EGQBpkIEuu.

[184] Gregory Benton, Marc Finzi, Pavel Izmailov, and Andrew Gordon Wilson. Learning invariances in neural networks. *Advances in Neural Information Processing Systems*, 2020, 2020.

[185] Difan Zou, Yuan Cao, Yuanzhi Li, and Quanquan Gu. The benefits of mixup for feature learning. In *International Conference on Machine Learning*, pages 43423–43479. PMLR, 2023.

[186] Xingyi Yang, Daquan Zhou, Songhua Liu, Jingwen Ye, and Xinchao Wang. Deep model reassembly. *Advances in neural information processing systems*, 35:25739–25753, 2022.

[187] Xingyi Yang, Jingwen Ye, and Xinchao Wang. Factorizing knowledge in neural networks. In *European Conference on Computer Vision*, pages 73–91. Springer, 2022.

[188] Kento Nozawa and Issei Sato. Empirical evaluation and theoretical analysis for representation learning: A survey. *arXiv preprint arXiv:2204.08226*, 2022.

[189] Evgenii Nikishin, Max Schwarzer, Pierluca D'Oro, Pierre-Luc Bacon, and Aaron Courville. The primacy bias in deep reinforcement learning. In *International conference on machine learning*, pages 16828–16847. PMLR, 2022.

[190] Ghada Sokar, Rishabh Agarwal, Pablo Samuel Castro, and Utku Evci. The dormant neuron phenomenon in deep reinforcement learning. In *International Conference on Machine Learning*, pages 32145–32168. PMLR, 2023.

[191] Saurabh Kumar, Henrik Marklund, and Benjamin Van Roy. Maintaining plasticity via regenerative regularization. *arXiv preprint arXiv:2308.11958*, 2023.

[192] Clare Lyle, Zeyu Zheng, Evgenii Nikishin, Bernardo Avila Pires, Razvan Pascanu, and Will Dabney. Understanding plasticity in neural networks. In *International Conference on Machine Learning*, pages 23190–23211. PMLR, 2023.

[193] Evgenii Nikishin, Junhyuk Oh, Georg Ostrovski, Clare Lyle, Razvan Pascanu, Will Dabney, and André Barreto. Deep reinforcement learning with plasticity injection. *Advances in Neural Information Processing Systems*, 36, 2024.

[194] Clare Lyle, Zeyu Zheng, Khimya Khetarpal, James Martens, Hado van Hasselt, Razvan Pascanu, and Will Dabney. Normalization and effective learning rates in reinforcement learning. *arXiv preprint arXiv:2407.01800*, 2024.

[195] Jordan Ash and Ryan P Adams. On warm-starting neural network training. *Advances in neural information processing systems*, 33:3884–3894, 2020.

[196] Zaheer Abbas, Rosie Zhao, Joseph Modayil, Adam White, and Marlos C Machado. Loss of plasticity in continual deep reinforcement learning. In *Conference on Lifelong Learning Agents*, pages 620–636. PMLR, 2023.

[197] Alex Krizhevsky, Ilya Sutskever, and Geoffrey E Hinton. Imagenet classification with deep convolutional neural networks. *Advances in neural information processing systems*, 25:1097–1105, 2012.

[198] Byungchan Ko and Jungseul Ok. Time matters in using data augmentation for vision-based deep reinforcement learning. *arXiv preprint arXiv:2102.08581*, 2021.

[199] Aditya Sharad Golatkar, Alessandro Achille, and Stefano Soatto. Time matters in regularizing deep networks: Weight decay and data augmentation affect early learning dynamics, matter little near convergence. *Advances in Neural Information Processing Systems*, 2019.

[200] Abhimanyu Dubey, Abhinav Jauhri, Abhinav Pandey, Abhishek Kadian, Ahmad Al-Dahle, Aiesha Letman, Akhil Mathur, Alan Schelten, Amy Yang, Angela Fan, et al. The llama 3 herd of models. *arXiv preprint arXiv:2407.21783*, 2024.

[201] Roya Firoozi, Johnathan Tucker, Stephen Tian, Anirudha Majumdar, Jiankai Sun, Weiyu Liu, Yuke Zhu, Shuran Song, Ashish Kapoor, Karol Hausman, et al. Foundation models in robotics: Applications, challenges, and the future. *The International Journal of Robotics Research*, page 02783649241281508, 2023.

[202] Moo Jin Kim, Karl Pertsch, Siddharth Karamcheti, Ted Xiao, Ashwin Balakrishna, Suraj Nair, Rafael Rafailov, Ethan Foster, Grace Lam, Pannag Sanketi, et al. Openvla: An open-source vision-language-action model. *arXiv preprint arXiv:2406.09246*, 2024.

[203] Yao Mu, Qinglong Zhang, Mengkang Hu, Wenhai Wang, Mingyu Ding, Jun Jin, Bin Wang, Jifeng Dai, Yu Qiao, and Ping Luo. Embodiedgpt: Vision-language pre-training via embodied chain of thought. In A. Oh, T. Naumann, A. Globerson, K. Saenko, M. Hardt, and S. Levine, editors, *Advances in Neural Information Processing Systems*, volume 36, pages 25081–25094. Curran Associates, Inc., 2023. URL https://proceedings.neurips.cc/paper_files/paper/2023/file/4ec43957eda1126ad4887995d05fae3b-Paper-Conference.pdf.

[204] Zhiyuan Li, Yanfeng Lu, Yao Mu, and Hong Qiao. Cog-ga: A large language models-based generative agent for vision-language navigation in continuous environments. *arXiv preprint arXiv:2409.02522*, 2024.

[205] Yueen Ma, Zixing Song, Yuzheng Zhuang, Jianye Hao, and Irwin King. A survey on vision-language-action models for embodied ai. *arXiv preprint arXiv:2405.14093*, 2024.

[206] Grace Tang, Swetha Rajkumar, Yifei Zhou, Homer Rich Walke, Sergey Levine, and Kuan Fang. Kalie: Fine-tuning vision-language models for open-world manipulation without robot data. *arXiv preprint arXiv:2409.14066*, 2024.

[207] Rafael Figueiredo Prudencio, Marcos ROA Maximo, and Esther Luna Colombini. A survey on offline reinforcement learning: Taxonomy, review, and open problems. *IEEE Transactions on Neural Networks and Learning Systems*, 2023.

[208] Denis Tarasov, Vladislav Kurenkov, Alexander Nikulin, and Sergey Kolesnikov. Revisiting the minimalist approach to offline reinforcement learning. *Advances in Neural Information Processing Systems*, 36, 2024.

[209] Seunghyun Lee, Younggyo Seo, Kimin Lee, Pieter Abbeel, and Jinwoo Shin. Offline-to-online reinforcement learning via balanced replay and pessimistic q-ensemble. In *Conference on Robot Learning*, pages 1702–1712. PMLR, 2022.

[210] Junsu Kim, Seohong Park, and Sergey Levine. Unsupervised-to-online reinforcement learning. *arXiv preprint arXiv:2408.14785*, 2024.

[211] Mitsuhiko Nakamoto, Simon Zhai, Anikait Singh, Max Sobol Mark, Yi Ma, Chelsea Finn, Aviral Kumar, and Sergey Levine. Cal-ql: Calibrated offline rl pre-training for efficient online fine-tuning. *Advances in Neural Information Processing Systems*, 36, 2024.

[212] Yang Yue, Bingyi Kang, Xiao Ma, Zhongwen Xu, Gao Huang, and Shuicheng Yan. Boosting offline reinforcement learning via data rebalancing. *arXiv preprint arXiv:2210.09241*, 2022.

[213] Nathan Lambert, Markus Wulfmeier, William Whitney, Arunkumar Byravan, Michael Bloesch, Vibhavari Dasagi, Tim Hertweck, and Martin Riedmiller. The challenges of exploration for offline reinforcement learning. *arXiv preprint arXiv:2201.11861*, 2022.

[214] Xiaoyu Wen, Xudong Yu, Rui Yang, Chenjia Bai, and Zhen Wang. Towards robust offline-to-online reinforcement learning via uncertainty and smoothness. *arXiv preprint arXiv:2309.16973*, 2023.

[215] Hongjoon Ahn, Jinu Hyeon, Youngmin Oh, Bosun Hwang, and Taesup Moon. Reset & distill: A recipe for overcoming negative transfer in continual reinforcement learning. *arXiv preprint arXiv:2403.05066*, 2024.

[216] Bhairav Mehta, Manfred Diaz, Florian Golemo, Christopher J Pal, and Liam Paull. Active domain randomization. In *Conference on Robot Learning*, pages 1162–1176. PMLR, 2020.

[217] Xiaoyu Chen, Jiachen Hu, Chi Jin, Lihong Li, and Liwei Wang. Understanding domain randomization for sim-to-real transfer. *arXiv preprint arXiv:2110.03239*, 2021.